On Boundary Value Problems of the Ideal-Fluid Thermocline*

RUI XIN HUANG

Department of Physical Oceanography, Woods Hole Oceanographic Institution, Woods Hole, Massachusetts

(Manuscript received 2 July 1987, in final form 3 November 1987)

ABSTRACT

Recent developments of ideal-fluid thermocline models are briefly reviewed. Using density coordinates, boundary value problems are formulated for the ideal-fluid thermocline with continuous stratification. Ekman pumping and surface density are specified as the upper boundary conditions. No flow is permitted through the ocean's eastern boundary nor its bottom. Each water column is divided into three parts, i.e., the stagnant abyssal water with specified stratification, the unventilated thermocline with its potential vorticity specified, and the ventilated thermocline with its potential vorticity determined by a global dynamic balance. The unventilated thermocline is further divided into the shallow and deep parts, potential vorticity is specified a priori for the latter; however, for the former, potential vorticity has to be chosen in the process of calculating the solution so as to make the solution self-consistent.

Numerical integration of the ideal-fluid thermocline equations is reduced to repeatedly integrating a second-order ordinary differential equation at each station. This integration process reveals the nonlinear interaction between the ventilated and unventilated thermocline and sheds light on the long-pursued question of how the potential vorticity field is determined in the ventilated thermocline of a continuously stratified ocean. A numerical example shows the three-dimensional circulation pattern of a wind-driven ocean interior with continuous stratification, including a subtropical gyre and a subpolar gyre.

The novel contributions in this study are formulating the suitable boundary value problems of the continuously stratified thermocline equations and solving these problems numerically.

1. Introduction

A primary goal of large-scale ocean circulation theory has been to understand the thermocline structure. There has been a lengthy debate over the role and relative importance of advection and diffusion in determining the thermocline structure in the open ocean. In particular, the analyses of Welander (1959) and Robinson and Stommel (1959) represented two different idealizations. Welander emphasized the importance of density advection but ignored diffusion. Robinson and Stommel emphasized vertical diffusion but only took part of the convection into account.

There is no question about the vital importance of mixing/friction in the dynamics of the general circulation within a closed basin. However, Welander proposed an idealized ocean model in which all these mixing/friction processes were concentrated within the mixed layer on the top, and the western boundary region and the interior flow was free of mixing/friction. Accordingly, the ideal-fluid theory was applied for calculating the lowest-order interior solution with the mixing/friction processes left as higher-order dynamics to be matched on the boundaries. After calculating the lowest-order interior solution, the real oceanic circulation could be seen much more clearly as the wave/turbulence processes are superimposed on this basic flow.

For a long time Welander's approach has been much favored among theoretical modelers due to its simplicity. The corresponding theory is called the ideal-fluid thermocline and the governing equation is called the ideal-fluid thermocline equation. The ideal-fluid thermocline equation can be written in the form of a first-order partial differential equation system or a single third-order partial differential equation (the M-equation, Welander, 1959). Although the ideal-fluid thermocline equation has a seemingly simple form, it is a highly nonlinear system of a special type. Huang (1984, 1986, HH hereafter) made a preliminary study of this system and classified it as a non-strict hyperbolic system. In fact, the characteristics of the ideal-fluid thermocline equation satisfy

$$\Phi_z{}^3(u\Phi_x + v\Phi_y + w\Phi_z) = 0,$$

where $\Phi(x, y, z)$ is the characteristic manifold, (u, v, w) are velocity components on the (x, y, z) coordinates. The first factor means z = constant is a triple characteristic surface. The second factor means a streamline is a characteristic. Therefore, this system is a highly

* Woods Hole Oceanographic Institution Contribution No. 6636.

Corresponding author address: Dr. Rui Xin Huang, Woods Hole Oceanographic Institution, Woods Hole, MA 02543.

degenerated hyperbolic system. The mathematical properties of this system are still largely unknown, and no well-posed boundary value problem of the ideal-fluid thermocline equation in a closed basin has been discussed before.

In spite of the mathematical difficulties, theoretical models guided by physical intuition have yielded much information about the nonlinear dynamics. Many of the theoretical models developed in the 1960s feature similarity solutions. The limitations of similarity solutions have long been recognized (e.g., see Veronis, 1969). After a period of relatively low activity in the 1970s, theoretical models aimed at nonsimilarity solutions became popular.

Rhines and Young (1982, RY hereafter) showed how the potential vorticity field could be determined within closed streamlines in the unventilated thermocline. Their approach combined the ideal-fluid motion with an infinitesimal mixing by eddies and gave a unique solution with potential vorticity homogenized. Luyten et al. (1983, LPS hereafter) applied the idea of purely density convection to a layered model and successfully overcame the original difficulty of determining the potential vorticity functional in Welander's (1971) model. In a layered discretization, the complicated partial differential equations became a set of algebraic equations. Therefore, the model provides a straightforward, though perhaps tedious (if the number of layers is large), solution for the ventilated thermocline. Pedlosky and Young (1983, PY hereafter) combined these two approaches into a model of semi-continuous stratification. Despite much effort to formulate a model of truly continuous stratification, no clear-cut solution has been reported.

Huang (1984, 1986) patched together different forms of potential vorticity and reproduced a three-dimensional structure with continuous stratification similar to observations. The model is only a diagnostic model since potential vorticity is specified a priori. Although the upper and lower density conditions and Ekman pumping condition are satisfied, the model can satisfy the no-flow lower boundary condition only in an asymptotical sense, i.e., by adjusting many parameters.

Several new similarity solutions have been published recently. Janowitz (1986) and Killworth (1987) showed some exact, closed-form analytical solutions in similarity form. Young and Ierley (1986) discussed the no-flux boundary condition at the eastern wall by using a new family of similarity solutions. Although these new solutions are much better than the previous ones, there is always the same old question: Can these solutions satisfy these general boundary conditions.

The answer seems definitely negative. A similarity solution is useful when there is no natural length scale in the problem. For a closed basin many boundary conditions applied to the model imply many intrinsic length scales. By assuming a specific form of similarity, there is a special constraint over the solution and it will not be a general solution which can satisfy the most general boundary conditions.

The eastern boundary condition has been a topic of discussion. Both Young and Ierley (1986) and Killworth (1987) used a no-flux condition at the eastern boundary. The same boundary condition is used in the present model. As will be shown later, however, this kind of eastern boundary condition is associated with some intrinsic singularity.

Young and Ierley also tried to emphasize the so-called "weak" solution for the ideal-fluid thermocline equation. They considered a discontinuity in density as weak solutions. It seems useful to distinguish these weak solutions and the weak solutions with which we are familiar from some well-known totally hyperbolic systems. There are examples in two-dimensional gas dynamics in which a weak discontinuity develops from a totally continuous upstream boundary condition (Courant and Friedrichs, 1948). The examples Young and Ierley used for interior density discontinuity were from LPS and PY. However, the density discontinuity in these two cases can be traced back to the western boundary or upper boundary; they were not created along the streamlines.

Although all these solutions with density discontinuity are perfectly legitimate solutions for the ideal-fluid thermocline equation, it does not mean there can be no solution with truly continuous stratification in the interior ocean.

There has been also some argument whether a level of no motion can exist in an ideal-fluid (Olbers and Willebrand, 1984). At that time it was unclear what the correct lower boundary conditions were for the ideal-fluid thermocline equation.

In fact, within the past 30 years, since the ideal-fluid thermocline was formulated, it was unclear how to formulate appropriate boundary value problems for the ideal-fluid thermocline equation. Welander (1971) pointed out that potential vorticity and the Bernoulli function are conserved along a streamline. He suggested the choice of some form of potential vorticity function, thus turning the original partial differential equation into a second-order ordinary differential equation. The major conceptual difficulty was that a second-order ordinary differential equation can only satisfy two boundary conditions. Thus, it was obscure how this process can lead to a solution that satisfies many boundary conditions. HH went one step further by constructing solutions which can satisfy three vertical boundary conditions and some lateral boundary conditions. However, complete formulations of boundary value problems are still lacking.

To answer all these questions, we need a solution for the ideal-fluid thermocline with continuous stratification. Continuous density boundary conditions will apply to all boundaries and thus eliminate the possibility of a density jump being advected into the interior. Our model will parallel the LPS and PY models. In

fact, we will formulate boundary value problems in density coordinates including LPS and PY models as special cases. By constructing continuous solutions, we prove the existence of continuously stratified solutions and the surface of no motion, a surface which separates the moving water from the stagnant abyssal water. In a sense, our model is a computer extension of the LPS model. However, instead of doing all these hard algebraic manipulations of layered models by human brain, we use finite difference in density coordinates and our modern slave, a PC, to do the job for us.

Section 2 is devoted to the description of the model. First, we classify four types of water in the model, i.e., the stagnant abyssal water, the deep unventilated thermocline, the shallow unventilated thermocline, and the ventilated thermocline. Second, we discuss the ventilation ratio and estimate how much water is really ventilated by Ekman pumping. Third, the basic equations and the corresponding boundary conditions are transformed into density coordinates. Several boundary value problems of the ideal-fluid thermocline equation are formulated in section 3. In these formulations, the problem of solving the ideal-fluid thermocline equation is reduced to repeatedly solving free boundary value problems of a second-order ordinary differential equation in the density coordinate. These free boundary value problems turn into simpler fixed boundary value problems or even closed analytical solutions when the deep unventilated thermocline has a constant potential vorticity as will be shown in section 4. A numerical example of a two-gyre circulation is presented in section 5 with some interesting maps. In general cases, the upper surface density is a function of x and y coordinates, and there can be weak flux across the eastern boundary. Boundary value problems formulated for these cases are discussed in section 6. Finally, we conclude in section 7 with topics for further study.

2. Description of the model

A continuously stratified ocean is confined within a rectangular basin on a β-plane. The upper surface of the model ocean is located at the bottom of an Ekman layer where water is pumped down into (or up from) the interior ocean. The ocean has a flat bottom with no topography. The northern, southern, and the intergyre boundaries of the basin are latitude circles ($y = y_n$, $y = y_s$, $y = y_0$), which are coincident with the zero-Ekman-pumping lines. A further assumption of no-water-mass-exchange across these latitudes is made in the model. This assumption is a choice of simplification rather than necessity; it is also a choice consistent with these boundary conditions (see HH). For simplicity, the density at the base of the mixed layer is assumed to be x-independent in the subtropical gyre. Figure 1 shows a schematic picture of the subtropical basin.

The eastern boundary of the ideal-fluid thermocline is connected with some kind of singularity and the corresponding boundary conditions can be either with flux or without. A no-flux condition is much easier to handle in a simple theoretical model, and it is the choice made in this study. It is readily shown that with such an eastern boundary condition the surface line along the eastern wall is a singular line where all isopycnals in the ventilated thermocline outcrop and meridional

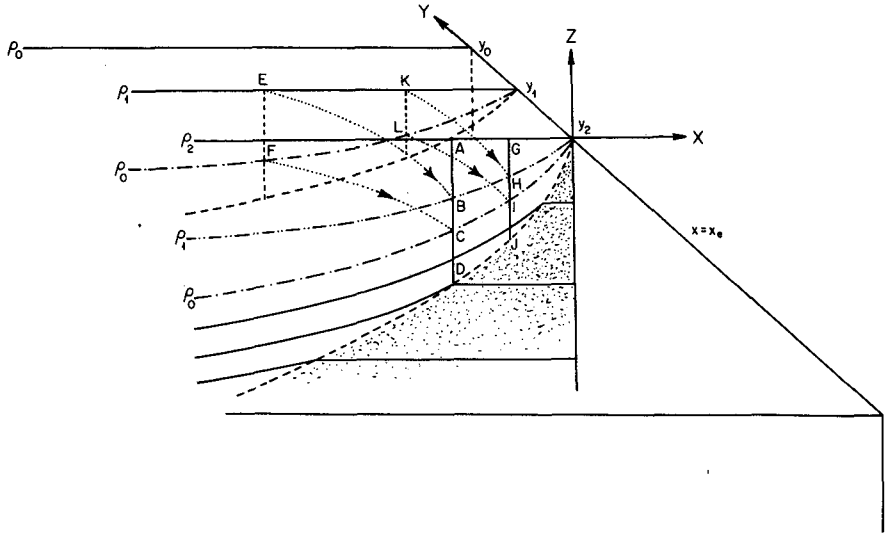

FIG. 1. Schematic picture of a subtropical basin. At the intergyre boundary $y = y_0$, $w_e = 0$ and $\rho_s = \rho_0$. At section y_2 the stratification of the ocean is depicted: the ventilated thermocline with $\rho < \rho_0$, the unventilated thermocline with $\rho > \rho_0$, and the stagnant abyssal water (shadow zone) adjacent to the eastern boundary.

velocity is unbounded (e.g., Young and Ierley, 1986). Nevertheless, it is readily seen that the vertically integrated meridional mass flux remains finite (equal to the Sverdrup flux). Boundary value problems with a general eastern boundary condition will be discussed in section 6.

a. Ventilated and unventilated thermoclines

In the early stages of thermocline theory, most theoretical models were similarity solutions, which made no distinction between different types of water in the circulation. During the past five years, it has become very clear that the thermocline consists of several domains that are quite different in their dynamic nature. Accordingly, each water column in a subtropical gyre can be divided into three parts vertically: 1) on the top, the ventilated thermocline—water comes from Ekman pumping over the upper surface; 2) in the middle depth, the unventilated thermocline—water comes from the western boundary outflow or northern/southern boundary; since a no-flux assumption has been applied to the northern, southern and intergyre boundaries in the model, outflow from the western boundary is the sole source of water in the unventilated thermocline; by definition, the unventilated thermocline has no contact with the Ekman layer within the subtropical gyre interior; 3) on the bottom, the abyssal water, which is assumed to be stagnant in the model.

Ventilated and unventilated thermoclines have quite different sources and thus drastically different natures. However, within the context of a layered model it is not always clear whether a water parcel should be classified as ventilated or unventilated. For a steady, continuously stratified model, it is crucial to make the distinction between the two types of water. All water coming from the western boundary (below the upper surface!) belongs to the unventilated thermocline, while the ventilated thermocline is strictly limited to the water which comes directly from Ekman pumping specified over the upper surface.

Accordingly, all moving water in a subpolar gyre interior belongs to the unventilated thermocline. Although the upper part of a water column can reach the base of the mixed layer, these water parcels do come from the western boundary outflow, thus they belong to the unventilated thermocline.

Since we assume that the upper surface density distribution in the subtropical basin is independent of x and increases northward, therefore, it is obvious that water having density larger than ρ_0 (the surface density at the intergyre boundary) must be in the unventilated thermocline. At first, this $\rho = \rho_0$ isopycnal interface seems an appropriate interface between the ventilated and unventilated thermocline. A close examination, however, reveals that even within the density range $\rho < \rho_0$ there may be a substantial portion of water that comes from the western boundary and thus belongs to the unventilated thermocline (see HH and Rhines, 1986). Figure 2 depicts the relative contribution of the unventilated thermocline on two isopycnal surfaces. Figure 2a shows a warm isopycnal surface on which the shaded area represents the unventilated thermocline which is less important here. This area was called a "pool" in the LPS model. It should be noticed that water in the top part of a column in this area is ventilated; therefore, resolving the interaction between the ventilated and the unventilated thermoclines in this area becomes crucially important in a continuous model. As an example, Fig. 2b shows the streamline pattern on an isopycnal surface close to ρ_0. The unventilated portion (or the pool area in LPS's terminology) occupies a major portion of the circulation. Obviously, as ρ increases toward ρ_0, all water must come from the western boundary outflow and belong to the unventilated thermocline.

It is clear from Fig. 2b that ignoring this pool area will leave a major portion of a subtropical gyre unresolved. As the number of layers in a model increases, resolving the dynamics of this pool becomes an essential requirement for the global structure. For a continuous model, therefore, specifying some additional information is an essential boundary condition along the western boundary. HH discussed the mathematical properties of the ideal-fluid thermocline equation and argued that information was needed wherever fluid came into the domain of the study. In the present model, there are only two boundaries through which water can come into the domain of study. First, water comes from the upper surface where both density and vertical velocity (Ekman pumping velocity) have been specified. Second, water comes from the western boundary. It is our major assumption in the model that, in addition to the density, some additional information has to be specified for these water particles. We propose to specify the functional form of potential vorticity in connection with density and the Bernoulli function. This is an extension from the combined model by PY. It is still unclear now whether some other information can be used instead of the potential

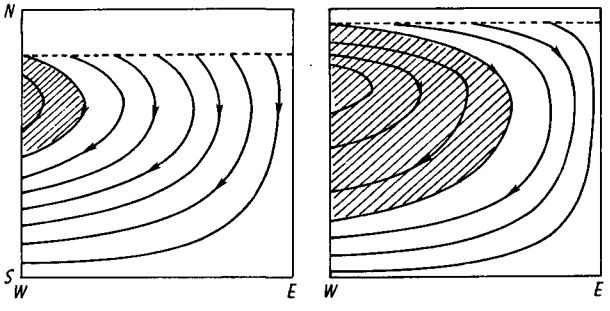

FIG. 2. Schematic streamline pattern on two isopycnal surfaces showing the boundary between the ventilated thermocline and the shallow unventilated thermocline (pool region).

vorticity function. Nevertheless, the requirement of specifying information in addition to the density is an essential boundary condition.

As one moves southward, this pool region gradually shrinks and eventually disappears. This difference in specifying boundary conditions for the northern and southern parts of the western boundary is a result of the mathematical properties of the so-called nonstrict hyperbolic system (HH).

In the following analysis an unventilated thermocline with density smaller than ρ_0 will be called the shallow unventilated thermocline, while that with density larger than ρ_0 will be called the deep unventilated thermocline. The potential vorticity functions for these two parts of the thermocline can be chosen differently because these functions can be piecewise continuous anyway.

b. *The ventilation ratio*

Rhines (1986) introduced a recirculation index, which actually indicated the ratio between the ventilated and unventilated thermocline. His estimation was based on a simple analysis of a meridional section. This ratio is meaningless for a subpolar gyre, thus our attention here is focused on a subtropical gyre. Since the overall importance is that of distinguishing the ventilated thermocline from the unventilated one, it seems worthwhile to calculate the exact ratio of the two types of water.

The wind forcing is assumed to be purely zonal, thus the volume flux in the Ekman layer is purely meridional. The corresponding Ekman fluxes entering from the northern and southern boundaries of a subtropical gyre are

$$M_{E0} = L(\tau/f)_{y=y_0}/\rho \tag{2.1}$$

$$M_{Es} = -L(\tau/f)_{y=y_s}/\rho \tag{2.2}$$

where τ is the wind stress, f is the Coriolis parameter, y_0 and y_s are the northern and southern boundaries, and L is the west–east extent of the basin. The total meridional volume flux, below the Ekman layer, is

$$M_{\text{int.}} = fw_eL/\beta = -(fL/\rho\beta)d(\tau/f)/dy. \tag{2.3}$$

Assume the wind stress takes the form

$$\tau = -(\tau_0 f(y)/f_m)\cos[\pi(y - y_s)/(y_0 - y_s)] \tag{2.4}$$

where $f_m = f(y_m)$ and $y_m = (y_s + y_0)/2$ is the midlatitude of the basin. The interior meridional volume flux reaches a maximum, $M_{\text{int.}m}$, (absolute value) at $y = y_m$ where the wind stress is zero and the Ekman flux is also zero. Therefore, the total volume flux crossing the western boundary south of $y = y_m$ is the sum of $|M_{\text{int.}m}|$ and M_{Es}, i.e.,

$$\begin{aligned} M_w &= -M_{\text{int.}}|_{y=y_m} + M_{Es} \\ &= \tau_0 L/\rho \cdot [1/f_m + \pi/\beta(y_0 - y_s)], \end{aligned} \tag{2.5}$$

while the total volume flux of the ventilated thermocline water (equal to the total volume flux of Ekman flux entering the region) is

$$M_E = 2\tau_0 L/\rho f_m. \tag{2.6}$$

We define the ventilation ratio as

$$R_c = \frac{\text{Volume flux in ventilated thermocline}}{\text{Total volume flux in thermocline}}. \tag{2.7}$$

Therefore, we have

$$R_c = 2[\pi f_m/\beta(y_0 - y_s) + 1]^{-1}. \tag{2.8}$$

For a typical subtropical gyre, $f_m = 8.37 \times 10^{-5}$ s^{-1}, $\beta = 1.875 \times 10^{-13}$ s^{-1} cm^{-1}, $y_0 - y_s = 2 \times 10^8$ cm, thus $R_c = 1{:}4.0$. This is the same value determined from observation (Rhines, 1986). (If one defines the ventilation ratio by calculation within the northern half of the subtropical gyre, this ratio becomes 1:8.0 in the model.) Accordingly, only a rather small portion of the water in a gyre actually comes from the Ekman pumping, while most water comes from the western boundary outflow. Therefore, even if our model is successful in determining the potential vorticity for the ventilated thermocline, this is only true for less than 25 percent of the total water; the rest of it must be specified a priori in the model. It may seem a disappointment for theoreticians who are enthusiastic about the ideal-fluid thermocline. But this is as far as we can get now.

c. *The basic equations in density coordinates*

The ideal-fluid thermocline equation consists of a nonlinear system which has a much simpler form in density coordinates (e.g., Robinson, 1965; Hodnett, 1978; Killworth, 1987). However, part of what we have gained in simplifying the form of the equations is lost because we must deal with some free boundary conditions. In density coordinates, the Bernoulli function

$$B = P + \rho gz \tag{2.9}$$

plays the role of the basic dependent variable. The hydrostatic relation becomes

$$B_\rho = gz \tag{2.10}$$

where subscript ρ denotes the derivative with respect to ρ hereafter. Differentiating (2.10) one more time gives

$$B_{\rho\rho} = gz_\rho. \tag{2.11}$$

This is the principal equation for the ideal-fluid thermocline in density coordinates. It is our major concern in this study to formulate suitable boundary value problems for this equation.

By introducing potential vorticity

$$q = f\rho_z, \tag{2.12}$$

(2.11) becomes

$$B_{\rho\rho} = fg/q(B, \rho). \tag{2.13}$$

For the ideal-fluid thermocline q is a function of the Bernoulli function and density (Welander, 1971); $q = Q(B, \rho)$. By assuming specific forms of Q, solutions to the basic equation (2.13) have been found which can satisfy different sets of boundary conditions (e.g., Welander, 1971; Janowitz, 1986; Killworth, 1987). By patching together different forms of potential vorticity functions, HH reproduced a global structure of subtropical–subpolar gyres in a basin interior.

Our primary interest, however, is to examine how this potential vorticity function for the ventilated thermocline is determined by boundary conditions specified at all boundaries. Since there has not been such an example, our goal is rather moderate. We want to formulate appropriate boundary value problems for the ideal-fluid thermocline and show just one example of a boundary value problem which yields a reasonable solution. Further manipulation and extension shall certainly give more possible choices and better results.

d. Boundary conditions

We assume that

$$\rho_s = \rho_0, \quad B^s = 0, \quad w_e = 0 \quad \text{at} \quad y = y_0, \tag{2.14}$$

where ρ_s and B^s are the density and Bernoulli function at the upper surface, $y = y_0$ is the intergyre boundary.

At the western boundary potential vorticity is specified as a function of Bernoulli function and density wherever water comes into the domain of study,

$$q = Q(B, \rho). \tag{2.15}$$

At the eastern boundary the upper surface density is assumed to be constant

$$\rho_s = \rho_0, \quad B^s = 0 \quad \text{at} \quad x = x_e \tag{2.16}$$

and the base of the moving water is coincident with the upper surface, i.e.,

$$\rho_b = \rho_0, \quad B_\rho(\rho_b) = 0 \quad \text{at} \quad x = x_e. \tag{2.17}$$

Below the upper surface the stratification of the stagnant abyssal water is given

$$\rho_z = \rho_z{}^a(\rho), \tag{2.18}$$

or equivalently

$$B^a = B^a(\rho), \quad B_\rho{}^a = B_\rho{}^a(\rho) \tag{2.19}$$

are given functions. These eastern boundary conditions in the model guarantee that $u \equiv 0$ at the eastern boundary.

The vertical boundary conditions need some discussion. Let us begin with the lower boundary conditions. The model includes a layer of stagnant abyssal water resting over a flat bottom. At the base of the moving water, i.e., the interface between the stagnant water and the unventilated thermocline, both the Bernoulli function and its derivative with respect to ρ are continuous

$$B^a = B^b \quad \text{at} \quad \rho = \rho_b(x, y) \tag{2.20a}$$

$$B_\rho{}^a = B_\rho{}^b \quad \text{at} \quad \rho = \rho_b(x, y) \tag{2.20b}$$

where $\rho_b = \rho_b(x, y)$ is a free boundary.

Since in density coordinates geostrophy, the vertical velocity, and mass conservation take the form

$$-\rho_0 f v = -B_x, \tag{2.21a}$$

$$\rho_0 f u = -B_y, \tag{2.21b}$$

$$w = u z_x + v z_y, \tag{2.22}$$

$$(u z_\rho)_x + (v z_\rho)_y = 0, \tag{2.23}$$

boundary conditions (2.20a, b) imply that

$$B_x = B_y = 0 \quad \text{at} \quad \rho = \rho_b(x, y), \tag{2.24}$$

and thus

$$u = v = w = 0 \tag{2.25}$$

at the base of the moving water.

Now let us discuss the upper boundary. Traditionally, two conditions are given over the upper boundary of a subtropical gyre

$$\rho = \rho_s \quad \text{at} \quad z = 0, \tag{2.26}$$

$$w = w_e \quad \text{at} \quad z = 0. \tag{2.27}$$

In density coordinates, the first condition turns out to be

$$B_\rho = 0 \quad \text{at} \quad \rho = \rho_s, \tag{2.28}$$

which is rather easy to apply in a model. For a subpolar basin, the upper surface density is unspecified; therefore, (2.28) becomes a free boundary condition

$$B_\rho = 0, \quad \text{at} \quad \rho = \rho_s \quad (\rho_s \text{ unknown}). \tag{2.28'}$$

There are two ways of applying condition (2.27). First, at the upper surface the density conservation equation can be turned into a first-order ordinary differential equation along its characteristics. For simplicity, assume that the upper surface density distribution is independent of x. Accordingly, on the upper surface the density conservation equation can be rewritten as

$$v = -w_e(z_\rho d\rho_s/dy)^{-1}. \tag{2.29}$$

Combining (2.29) with (2.21a), it follows that

$$B_x{}^s = -\rho_0 w_e q_s (d\rho_s/dy)^{-1} \tag{2.30}$$

which links the horizontal derivative of B^s to the potential vorticity at the upper surface. For a general upper surface density distribution, (2.30) can be written in a similar form by using characteristic coordinates. This approach has been successfully applied to cases where $B_x{}^s$ is finite at the eastern boundary (HH).

It is readily seen that (2.30) is equivalent to the Sverdrup relation in some earlier theoretical studies. For example, assuming

$$q = 1/F(\rho)B, \tag{2.31}$$

(2.30) becomes, upon integrating once,

$$B^2 = B_0^2 - 2\rho_0[F(\rho_s)d\rho_s/dy]^{-1}\int_0^x w_e dx, \quad (2.32)$$

which is equivalent to Eq. (2.21) in Killworth's study. Assumption (2.31) was motivated by analytical convenience rather than physical reasoning. This assumption cannot encompass the dynamical differences of the ventilated and unventilated thermoclines, thus failing to predict the correct structure.

In the present model, since a no-flux condition is assumed along the eastern boundary, both v and B_x^s are singular along the surface line at the eastern boundary. As a result, (2.30) is not suitable for starting the integration near the eastern wall. Instead, an integral condition can be used for numerical integration.

First, cross-differentiating (2.21a, b) and using (2.22), (2.23) gives

$$\beta v = f w_\rho / z_\rho, \quad (2.33)$$

which combines with (2.21a) to yield

$$B_x z_\rho = \rho_0 f^2 w_\rho / \beta. \quad (2.34)$$

Integrating over $[\rho_s, \rho_b]$

$$\rho_0 f^2 w_e/\beta = \int_{\rho_b}^{\rho_s} B_x z_\rho d\rho. \quad (2.35)$$

Substituting $B_{\rho\rho}/g$ for z_ρ and integrating by parts, one obtains

$$\rho_0 f^2 w_e/\beta = \frac{1}{g}\int_{\rho_s}^{\rho_b} (0.5B_\rho^2)_x d\rho, \quad (2.36)$$

where boundary conditions (2.28) and (2.24) have been used. Since $B_\rho = gz < 0$ except on the upper surface, Eq. (2.36) has a very clear meaning, i.e., $(dz/dx)_{\rho=\text{const}}$ has a sign different from w_e. In other words, isopycnals slope down westward in the subtropical gyre, while they slope up westward in the subpolar gyre. Equation (2.36) can be rewritten, after simple manipulation, as

$$-\int_{\rho_s}^{\rho_b} B_\rho^2 d\rho = (\rho_0 f^2 g/\beta)\int_x^{x_e} w_e dx + \int_x^{x_e} B_\rho^2(\rho_b) d\rho_b/dx \cdot dx, \quad (2.37)$$

where $\rho_b = \rho_b(x, y)$ is variable and eastern boundary conditions (2.16) and (2.17) have been used in deriving (2.37). Using (2.10), (2.37) can be reduced to

$$-\int_{\rho_s}^{\rho_b} Z^2 d\rho = (2\rho_0 f^2/g\beta)\int_x^{x_e} w_e dx + \int_x^{x_e} Z^2(\rho_b) d\rho_b/dx \cdot dx. \quad (2.37')$$

This is the Sverdrup relation in an integral form; its usefulness will be demonstrated in the following sections.

For a reduced gravity model the last term in (2.37) drops out. Since

$$\int_{\rho_b}^{\rho_s} B_\rho^2 d\rho \approx -\Delta\rho g^2 D^2, \quad (2.38)$$

where D is the layer depth, (2.37) degenerates to

$$D^2 = -(2\rho_0 f^2/g\beta\Delta\rho)\int_x^{x_e} w_e dx \quad (2.39)$$

which is the familiar formula for the layer depth of a reduced gravity model (assuming $D = 0$ at the eastern wall).

3. Boundary value problems for the ideal-fluid thermocline equation

The basic equations and boundary conditions for the ideal-fluid thermocline have been discussed in the previous section. Formulating suitable boundary value problems of the ideal-fluid thermocline and the procedure of solving the boundary value problems are our concern in this section. We will show that solving the ideal-fluid thermocline can be reduced to repeatedly integrating a second-order ordinary differential equation with some free boundary conditions.

a. Boundary value problems for a subtropical basin

The subtropical basin is divided into N west–east sections and the integration progresses section by section southward, starting from the northern boundary. At each section the integration goes westward station by station. At each station a two-point boundary value problem of a second-order ordinary differential equation is integrated by a shooting method. This process is depicted in Fig. 1.

For example, integration at section y_2 is underway only after integration on section y_1 has been completed. Integration at station A follows that at station G (though for boundary value problem B′, this is not necessary, see discussion below). After completion of integration at section y_1, a one-dimensional data array is stored in the computer memory for the functional relation $q = q(B, \rho_1)$ for $B = [0, B_w]$, where B_w is the Bernoulli function on the upper surface at the western end of this section. These data arrays can be used to provide a potential vorticity value wherever B and ρ are given. It is easy to see the connection between the LPS model and the present model in tracing the potential vorticity to the place where water enters the domain of study.

At each station, the integration is reduced to solving a two-point boundary value problem of a second-order ordinary equation. As discussed above, the base of the moving water is a free boundary with two boundary conditions

$$B = B^a(\rho_b) \quad \text{at} \quad \rho = \rho_b \quad (2.20a)$$

$$B_\rho = B_\rho{}^a(\rho_b) \quad \text{at} \quad \rho = \rho_b \tag{2.20b}$$

where both $B^a(\rho)$ and $B_\rho{}^a(\rho)$ are given functions. Now our task is to solve the second-order ordinary differential equation (2.13), i.e.,

$$B_{\rho\rho} = fg/q(B, \rho),$$

where $q(B, \rho)$ is a known function for $\rho > \rho_s$ either in the form of a specified function or data arrays of numerical results from previous steps, though $q(B, \rho_s)$ is still unknown. In addition, there is a fixed boundary condition at the upper surface (2.28)

$$B_\rho = 0 \quad \text{at} \quad \rho = \rho_s,$$

where $\rho_s = \rho_s(x, y)$ is given for a subtropical basin. Since (2.13) is of second order, it cannot be solved without an additional condition.

There are two possible choices, and, accordingly, two ways of formulating a suitable boundary condition for the ideal-fluid thermocline.

1) BOUNDARY VALUE PROBLEM A

Equation (2.13) and boundary conditions (2.28; 2.20a, b; 2.30) constitute a deterministic two-point boundary value problem, i.e.,

$$B_{\rho\rho} = fg/q(B, \rho), \tag{2.13}$$

$$B_\rho = 0 \quad \text{at} \quad \rho = \rho_s, \tag{2.28}$$

$$B = B^a(\rho_b) \quad \text{at} \quad \rho = \rho_b \quad (\rho_b \text{ unknown}), \tag{2.20a}$$

$$B_\rho = B_\rho{}^a(\rho_b) \quad \text{at} \quad \rho = \rho_b, \tag{2.20b}$$

$$B^s = B^s(x + \Delta x) + \Delta x w_e q_s (d\rho_s/dy)^{-1}, \tag{2.30'}$$

where B^s and q_s are the unknown Bernoulli function and potential vorticity at the sea surface, and (2.30') has been derived by rewriting (2.30) in a finite difference form. This problem can be solved with a shooting method and the Heun scheme (Mesinger and Arakawa, 1976) for the differential equation (2.13) as follows, see Fig. 1.

Assuming q_s given, (2.28, 2.30') give all the necessary information to start the integration downward. As the integration reaches point B, the corresponding potential vorticity value q can be determined by interpolation from data arrays generated from previous steps on section y_1, giving the first estimate of the Bernoulli function at point B. The integration continues to isopycnal ρ_b where the lower boundary conditions (2.20a, b) are specified. Since the first estimate of q_s is unlikely to give a solution satisfying (2.20a, b), the value of q_s is repeatedly adjusted until (2.20a, b) are met. Obviously, the integrating process can also be carried out upward and yields the same result. See discussion for boundary value problem B below.

This two-point boundary value problem is deterministic. The well-posedness of this problem is rather complicated. Due to its peculiar formulation, proof of the well-posedness is not of local nature at all. However, when the iterative process does converge, the Bernoulli function and potential vorticity at point A are determined and the integration process is moved westward to the next station, and so on.

There are two possible difficulties associated with this integration process. First, in the middle of the basin, the value of the Bernoulli function for density less than ρ_0 may exceed the maximum value of the Bernoulli function stored in the data arrays. Physically, this means that the corresponding water particles come from the western boundary, though their density is less than ρ_0. This is the shallow unventilated thermocline discussed in the previous section. Accordingly, the potential vorticity functional form has to be specified for this type of water. Since this water circulates in the upper ocean, its potential vorticity is unlikely to be homogenized. Specification of an appropriate functional form for these water particles also provides new degrees of freedom for the basin circulation.

Second, the surface line along the eastern wall is a singular line for the meridional velocity due to the specific eastern boundary condition applied in the model. As a result, $B_x{}^s$ is unbounded near the eastern wall and (2.30') is not suitable for starting the integration from the eastern wall. To overcome this difficulty, the following formulation can be used.

2) BOUNDARY VALUE PROBLEM B

Equation (2.13) and boundary conditions (2.28; 2.20a, b; 2.37) constitute a deterministic boundary value problem, i.e.

$$B_{\rho\rho} = fg/q(B, \rho), \tag{2.13}$$

$$B_\rho = 0 \quad \text{at} \quad \rho = \rho_s, \tag{2.28}$$

$$B = B^a(\rho_b) \quad \text{at} \quad \rho = \rho_b, \quad (\rho_b \text{ unknown}) \tag{2.20a}$$

$$B_\rho = B_\rho{}^a(\rho_b) \quad \text{at} \quad \rho = \rho_b, \tag{2.20b}$$

$$-\int_{\rho_s}^{\rho_b} B_\rho{}^2 d\rho = 2\rho_0 f^2 g\beta^{-1} \int_x^{x_e} w_e dx + \int_x^{x_e} B_\rho{}^2(\rho_b) d\rho_b/dx \cdot dx. \tag{2.37}$$

This problem can be solved by a shooting method starting from a guessed density $\rho = \rho_b$, since both B and B_ρ at $\rho = \rho_b$ can be determined by the given functions $B^a(\rho)$ and $B_\rho{}^a(\rho)$. Equation (2.13) is integrated upward for $\rho_b \geq \rho \geq \rho_s$. Although q_s is unknown, it can be determined such that boundary condition (2.28) will be met at the surface. The value of ρ_b must be repeatedly adjusted such that integration condition (2.37) will be met for the final set of parameters.

This formulation uses the integrated formula of the Sverdrup relation and thus avoids the singularity associated with the eastern boundary appearing in the previous formulation. Otherwise, these two formula-

tions are very similar for the interior ocean, except that they begin at different ends of the same density interval.

Both formulations show the intrinsic nonlinear coupling between the ventilated and unventilated thermocline. The determination of the potential vorticity in the ventilated thermocline has been reduced to repeatedly integrating two-point boundary value problems of a second-order ordinary differential equation. All boundary conditions for a basinwide model play a role in this seemingly localized, vertical integration process. First, the eastern boundary condition is combined with the free boundary conditions at the interface between the moving and stagnant water. In the next section we will show that the assumption of a homogenized potential vorticity for water column with $\rho_b \geqslant \rho \geqslant \rho_0$ reduces this free boundary value problem to a simple fixed boundary condition at $\rho = \rho_0$. Second, the western boundary condition of specifying potential vorticity is used for both the deep unventilated thermocline with $\rho \geqslant \rho_0$ and the shallow unventilated thermocline with $\rho < \rho_0$ whenever inversion of the potential vorticity function reaches a Bernoulli function value outside the range of the ventilated water. Third, the upper surface density distribution is used as the end point of the vertical integration and the density gradient is used in (2.30′) for boundary value problem A. Finally, the Ekman pumping velocity is used either as a link between the potential vorticity and Bernoulli function at the upper surface, e.g., (2.30′), or as a vertical integration constraint (2.37).

The ideal-fluid thermocline equation has been classified as a non-strict hyperbolic system (HH). Our model shows the specific features of this system. As a non-strict hyperbolic system, the ideal-fluid thermocline model has properties similar to totally hyperbolic systems, such as: 1) Some physical quantities (i.e., potential vorticity, density and Bernoulli function) are conserved along streamlines which are characteristics of the system. 2) Two boundary conditions are specified where water particles enter the domain of study (i.e., ρ_s and w_e at the upper boundary, ρ and q at the western boundary). The system also possesses properties which do not belong to totally hyperbolic systems. For example, in the process of vertical integration at each station, all boundary conditions (including the eastern, western, upper and lower boundary conditions) are involved. Since no characteristic can link all these boundaries with moving water in the interior, the mechanism through which all boundary conditions affect the interior points is of non-strict hyperbolic nature. Our analysis here gives only a glimpse of the mathematical and physical nature of this non-strict hyperbolic system. Further study of this system is required.

b. Boundary value problem for a subpolar gyre

In a subpolar basin the Ekman pumping velocity is positive, i.e., water is sucked into the Ekman layer. Therefore, the formulation of boundary value problems may be different from the case of negative Ekman pumping velocity. In LPS, the upper surface density is determined by the outcropping line of individual layers. A working assumption was also made in the model that each layer is motionless until the one above it outcrops. Apparently, this assumption is unnecessary because water can be ventilated through the western boundary even before the individual layer touches the mixed layer directly. This is essential to models of continuous stratification, for example PY and HH.

Since all water particles in a subpolar basin come from the western boundary and have a density larger than ρ_0, they belong to the deep unventilated thermocline. Assuming the potential vorticity is a given function $q = q(B, \rho)$, the structure of the subpolar gyre can be determined by solving the following free boundary value problem.

BOUNDARY VALUE PROBLEM C

Equation (2.13) and the following boundary conditions constitute a boundary value problem for the ideal-fluid thermocline in a subpolar basin.

$$B_{\rho\rho} = fg/q(B, \rho), \tag{2.13}$$

$$B_\rho = 0, \quad \text{at} \quad \rho = \rho_s \quad (\rho_s \text{ unknown}) \tag{2.28′}$$

$$B = B^a(\rho_b), \quad \text{at} \quad \rho = \rho_b \quad (\rho_b \text{ unknown}) \tag{2.20a}$$

$$B_\rho = B_\rho{}^a(\rho_b) \quad \text{at} \quad \rho = \rho_b \tag{2.20b}$$

$$-\int_{\rho_s}^{\rho_b} B_\rho{}^2 d\rho = 2\rho_0 f^2 g\beta^{-1} \int_x^{x_e} w_e dx + \int_x^{x_e} B_\rho{}^2(\rho_b) d\rho_b/dx \cdot dx \tag{2.37}$$

where $B^a(\rho)$, $B_\rho{}^a(\rho)$ and $q(B, \rho)$ are all given functions, although they may be piecewise continuous.

The numerical solution of boundary value problem C is straightforward. The subpolar basin is divided into N latitude sections. At each section the integration starts from the eastern boundary where $\rho_s = \rho_b = \rho_0$ and marches westward station by station. At each station a shooting method is applied by starting from a first guess of ρ_b. From (2.20a, b) B and B_ρ at ρ_b can be calculated and used to start the integration upward. The integration stops at the free boundary $\rho = \rho_s$ where B_ρ crosses zero. The integration constraint (2.37) is checked to see whether the first guess of ρ_b is correct. This value ρ_b, then, can be repeatedly corrected to make the solution meet condition (2.37). The integrals in (2.37) can be calculated by some standard formula and (2.13) can be integrated by standard finite difference schemes.

This boundary value problem is deterministic. Therefore, for reasonable boundary conditions, such as $w_e(x, y)$, $q(B, \rho)$ and $B^a(\rho)$, the above process will give ρ_b and ρ_s at each station. The integration process

can be carried out at the next station to the west along the same section and so on.

A major difference between boundary value problem C and boundary value problem A or boundary value problem B is that now the integration at each section is independent of each other. This is a very convenient feature.

The well-posedness of this problem will be left for further study; here we want to point out some hidden features of this problem.

(i) Rearranging (2.37) as

$$\int_x^{x_e} B_\rho{}^2(\rho_b)d\rho_b/dx \cdot dx = -\int_{\rho_s}^{\rho_b} B_\rho{}^2 d\rho - 2\rho_0 f^2 g\beta^{-1} \int_x^{x_e} w_e dx,$$

it is readily seen that $d\rho_b/dx$ is generally negative in the subpolar gyre where w_e is non-negative. That means the base of the moving water slopes up eastward.

(ii) As pointed out in section 2, $(\partial z/\partial x)_{\rho=\text{const}} < 0$ ($w_e > 0$) for the moving water. Therefore $|q^h| < |q^a|$ is required as a consistent condition for the boundary value problem C. Physically, it is clear that the stratification in the moving water should be weaker than in the stagnant water because of the Ekman suction.

4. Solution with constant potential vorticity in the deep unventilated thermocline

We have formulated boundary value problems for the ideal-fluid thermocline in the previous section. Now we study some simple examples to show how to solve these boundary value problems. The simplest case is one of constant potential vorticity in the deep unventilated thermocline. As we will see, the free boundary value problem in the subtropical gyre reduces to a fixed boundary value problem for the same second-order ordinary differential equation. For the subpolar basin the free boundary value problem reduces to a simple analytical solution.

Specifically, the model consists of an ocean on a β-plane with the central latitude at $y = y_0$ where $f = f_0$. The abyssal water has a linear stratification $\rho_z{}^a = \text{const}$, thus

$$q^a = f\rho_z{}^a. \tag{4.1}$$

The deep unventilated thermocline has a constant potential vorticity (see RY)

$$q^h = f_0\rho_z{}^a \quad \text{for} \quad \rho_b \geqslant \rho \geqslant \rho_0. \tag{4.2}$$

First, we will examine the solution in the subtropical and subpolar gyre separately. Second, we will prove the continuity of the solution across the inter-gyre boundary.

a. Solution in the subtropical basin

Since the potential vorticity function for $\rho \geqslant \rho_0$ has been specified, our discussion will be focused on the determination of the potential vorticity for $\rho_0 \geqslant \rho \geqslant \rho_s$, where ρ_s is the upper surface density at a given station. In other words, we want to transfer boundary conditions (2.20a, b; 2.37) to the intermediate isopycnal $\rho = \rho_0$.

Assume that

$$B = B^0, \quad B_\rho = B_\rho{}^0 \quad \text{at} \quad \rho = \rho_0. \tag{4.3}$$

Integrating (2.13) downward with boundary conditions (4.3), one obtains

$$B_\rho = B_\rho{}^0 + fg(\rho - \rho_0)/q^h \tag{4.4}$$

$$B = B^0 + B_\rho{}^0(\rho - \rho_0) + fg(\rho - \rho_0)^2/2q^h. \tag{4.5}$$

According to the eastern boundary condition (2.16) and (2.17),

$$B^e = 0, \quad B_\rho{}^e = 0, \quad \text{at} \quad \rho = \rho_0;$$

thus the corresponding structure at the eastern wall is

$$B_\rho{}^e = fg(\rho - \rho_0)/q^a \tag{4.6}$$

$$B^e = fg(\rho - \rho_0)^2/2q^a. \tag{4.7}$$

Substituting (4.4) and (4.6) into (2.20b) gives

$$\rho_b - \rho_0 = B_\rho{}^0 q^a q^h / fg(q^h - q^a). \tag{4.8}$$

Substituting (4.5) and (4.7) into (2.20a) gives

$$B^0 = B_\rho{}^0 q^h q^a / 2fg(q^a - q^h). \tag{4.9}$$

Substituting (4.8) into (4.4), one obtains

$$B_\rho{}^b = B_\rho{}^0 q^h / (q^h - q^a). \tag{4.10}$$

Since $B_\rho = gz$ by definition, the above formula states that at each zonal section the depth of the base of the moving water is linearly proportional to the depth of the $\rho = \rho_0$ interface. Meanwhile (4.9) means the Bernoulli function on the ρ_0-isopycnal is proportional to the square of the interfacial depth. It is important to note that (4.8), (4.9) and (4.10) are independent of all upper boundary conditions.

It is easy to show that (4.10) is valid for more general cases where $\rho_z{}^a$ is not constant, but potential vorticity is homogenized on each isopycnal surface and thus q^h/q^a is a constant. Thus, (4.10) is an important relation describing the depth of penetration of a homogenized gyre.

Now the free boundary conditions (2.20a, b) at $\rho = \rho_b$ (unknown) become a fixed boundary condition (4.9) at $\rho = \rho_0$. After a solution is determined, the free boundary $\rho = \rho_b$ can be calculated from (4.8).

Similarly, (2.37) can be simplified in the present case. Using (4.4, 4.8, 4.10), one obtains

$$\int_{\rho_s}^{\rho_b} B_\rho{}^2 d\rho = -q^h B_\rho{}^{0^3}[1 - (1 - q^a/q^h)^{-3}]/3fg + \int_{\rho_s}^{\rho_0} B_\rho{}^2 d\rho \tag{4.11}$$

$$\int_x^{x_e} B_\rho{}^2(\rho_b) d\rho_b/dx \cdot dx = q^a B_\rho{}^{03}/3fg(q^a/q^h - 1)^3. \tag{4.12}$$

Substituting (4.11, 4.12) into (2.37) gives a final form

$$B_\rho{}^{03} q^h[1 - (1 - q^a/q^h)^{-2}]/3fg - \int_{\rho_s}^{\rho_0} B_\rho{}^2 d\rho = 2\rho_0 f^2 g\beta^{-1} \int_x^{x_e} w_e dx. \tag{4.13}$$

Again, this is a vertical integration constraint over the dynamical field. It is equivalent to the Sverdrup relation in many theoretical models. Assuming B_ρ is a linear function of ρ, (4.13) predicts that the depth of the ρ_0-isopycnal interface slopes down westward in proportion to $[(x_e - x)w_e]^{1/3}$.

Therefore, using the new boundary conditions (4.9) and (4.13), boundary value problems A and B become fixed boundary value problems in the following forms.

BOUNDARY VALUE PROBLEM A′

Equation

$$B_{\rho\rho} = fg/q(B, \rho) \tag{2.13}$$

with fixed boundary conditions:

$$B_\rho = 0 \quad \text{at} \quad \rho = \rho_s \tag{2.28}$$

$$B^s = B^s(x + \Delta x) + \Delta x w_e q_s (d\rho_s/dy)^{-1} \quad \text{at} \quad \rho = \rho_s \tag{2.30′}$$

$$B^0 = B_\rho{}^{02} q^h q^a / 2fg(q^a - q^h) \quad \text{at} \quad \rho = \rho_0 \tag{4.9}$$

BOUNDARY VALUE PROBLEM B′

Equation

$$B_{\rho\rho} = fg/q(B, \rho) \tag{2.13}$$

with fixed boundary conditions:

$$B_\rho = 0 \quad \text{at} \quad \rho = \rho_s \tag{2.27}$$

$$B^0 = B_\rho{}^{02} q^h q^a / 2fg(q^a - q^h) \quad \text{at} \quad \rho = \rho_0 \tag{4.9}$$

$$B_\rho{}^{03} q^h[1 - (1 - q^a/q^h)^{-2}]/3fg - \int_{\rho_s}^{\rho_0} B_\rho{}^2 d\rho = 2\rho_0 f^2 g\beta^{-1} \int_x^{x_e} w_e dx. \tag{4.13}$$

These two boundary value problems can be solved by a shooting method similar to the ways described in the previous section. For example, in boundary value problem B′, assuming a first guess of $B_\rho{}^0$, B^0 can be calculated by (4.9). Thus (2.13) can be integrated from ρ_0 to ρ_s. q_s can be determined by requiring (2.28) be met. Then (4.13) is checked out, repeatedly adjusting $B_\rho{}^0$ until (4.13) is met.

b. Solution in the subpolar basin

The vertical structure can be calculated by integrating (2.13) downward. At the upper surface

$$B_\rho = 0, \quad B^s \text{ (unknown)} \quad \text{at} \quad \rho = \rho_s \text{ (unknown)}. \tag{4.14}$$

Therefore, a simple integration in density coordinates gives the structure of the moving water

$$B_\rho = fg(\rho - \rho_s)/q^h \tag{4.15}$$

$$B = B^s + fg(\rho - \rho_s)^2/2q^h \tag{4.16}$$

where q^h is the constant potential vorticity specified in (4.2). At the base of the moving water B_ρ and B should match the values calculated from (4.6, 4.7), thus

$$\rho_b - \rho_0 = f(\rho_b - \rho_s)/f_0 \tag{4.17}$$

$$B^s = fg(f - f_0)(\rho_b - \rho_s)^2/2f_0^2\rho_z{}^a. \tag{4.18}$$

The integrals in (2.37) can be calculated exactly

$$\int_{\rho_s}^{\rho_b} B_\rho{}^2 d\rho = \frac{1}{3}(fg/f_0\rho_z{}^a)^2(\rho_b - \rho_s)^3 \tag{4.19}$$

$$\int_x^{x_e} B_\rho{}^2(\rho_b) d\rho_b/dx \cdot dx = -\frac{1}{3} ff_0^{-1}(fg/f_0\rho_z{}^a)^2(\rho_b - \rho_s)^3 \tag{4.20}$$

where the boundary conditions that $\rho_b = \rho_s = \rho_0$ at $x = x_e$ have been used. Substituting (4.19), (4.20) into (2.37), one finds

$$\rho_b - \rho_s = f_0[6\rho_0\rho_z{}^{a^2} w_e(x_e - x)/g\beta(f - f_0)]^{1/3}. \tag{4.21}$$

Using (4.21) both the Bernoulli function and density at the upper surface can be found

$$B^s = 0.5f[36\rho_0^2(f - f_0)q\rho_z{}^a w_e^2(x_e - x)^2/\beta^2]^{1/3} \tag{4.22}$$

$$\rho_s = \rho_0 + [6\rho_0\rho_z{}^{a^2}(f - f_0)^2 w_e(x_e - x)/q\beta]^{1/3}. \tag{4.23}$$

The base of the moving water is

$$z^b = B_\rho{}^b/g = f[6\rho_0 w_e(x_e - x)/g\beta\rho_z{}^a(f - f_0)]^{1/3}. \tag{4.24}$$

This solution was first discussed by PY. The analysis above shows that this is a special case of a general family of solutions.

c. Continuity of the solutions near $y = y_0$

When approaching the $y = y_0$ line from the subtropical interior, the second term in (4.13) is a higher order term compared with the Ekman pumping term, thus it can be omitted. We have the following approximations:

$$1 - (1 - q^a/q^h)^{-2} \approx -f_0^2\beta^{-2}(y - y_0)^{-2} \tag{4.25}$$

$$\int_x^{x_e} w_e dx \approx w_d(y - y_0)(x_e - x) \tag{4.26}$$

where

$$w_d = dw_e/dy|_{y=y_0}. \tag{4.27}$$

Thus (4.13) gives an estimation

$$B_\rho{}^0 \approx -[6\rho_0 g^2\beta w_d(x_e - x)/\rho_z{}^a]^{1/3}(y - y_0). \tag{4.28}$$

By (4.9) one obtains

$$B^0 \approx 0.5f(36\rho_0{}^2 g w_d{}^2\rho_z{}^a/\beta)^{1/3}(x_e - x)^{2/3}(y - y_0). \tag{4.29}$$

Furthermore, the base of the moving water is

$$Z^b \approx f(6\rho_0 w_d/g\beta^2\rho_z{}^a)^{1/3}(x_e - x)^{1/3}. \tag{4.30}$$

Now it is easily seen that, as $y \to y_0$ from the subpolar basin, (4.22) and (4.24) become the same as (4.29) and (4.30). Assuming w_d is continuous across $y = y_0$, both the Bernoulli function at the $\rho = \rho_0$ isopycnal interface and the base of the moving water are continuous at $y = y_0$. Furthermore, by differentiating (4.22), (4.29) with respect to y, one finds that

$$u^0 = -dB^0/dy/f\rho_0 = -0.5(36gw_d{}^2\rho_z{}^a/\beta\rho_0)^{1/3}(x_e - x)^{2/3} \tag{4.31}$$

is continuous and finite at $y = y_0$.

d. Consistent condition of the upper surface density distribution near the northern boundary of the subtropical gyre

For a boundary value problem of the ideal-fluid thermocline in a subtropical basin, the upper surface density distribution is needed as the upper boundary condition. At first, a natural choice for a simple theoretical model is to assume that the upper surface density is a linear function of y, at least near the intergyre boundary $y - y_0$, i.e.,

$$\rho = \rho_0 + (y - y_0)d\rho_s/dy, \tag{4.32}$$

where $d\rho_s/dy$ is a constant. However, a careful examination of the potential vorticity field reveals some inconsistency in the solution. For a section near $y = y_0$, the average potential vorticity of water above the ρ_0-isopycnal surface can be estimated by (4.28)

$$q = f_0\Delta\rho/\Delta z = -f_0 g d\rho_s/dy \cdot (y - y_0)/B_\rho{}^0$$
$$= f_0 d\rho_s/dy \cdot (g\rho_z{}^a/6\rho_0\beta w_d)^{1/3}(x_e - x)^{-1/3}. \tag{4.33}$$

Therefore, q is finite as $y \to y_0$, except near $x = x_e$ where q has a $-\frac{1}{3}$-power singularity. However, all streamlines within $y_0 - \epsilon \leqslant y \leqslant y_0$ and $\rho < \rho_0$ have to pass through the "bottle neck" on the eastern boundary and thus should have had an infinite potential vorticity even before they reach the eastern boundary. Thus all these water particles should have an infinite potential vorticity. This implies two important constraints.

First, the potential vorticity of the shallow unventilated thermocline cannot be chosen too arbitrarily because it should be infinite for the aforementioned water particles. Now, it is very clear that the dynamic character of the shallow unventilated thermocline is quite different from the deep unventilated thermocline, as the potential vorticity of the latter is not subjected to the same constraint.

Second, the potential vorticity of the ventilated thermocline should be infinite for the regime adjacent to the northern boundary of the subtropical gyre. To avoid an inconsistency in the model we discuss several possible remedies.

(i) A simple choice is to assume that the upper surface density distribution is different from a linear function near $y = y_0$. Basically, to have a consistent solution, the density gradient should be singular at $y = y_0$, i.e.,

$$d\rho_s/dy = \infty \quad \text{at} \quad y = y_0. \tag{4.34}$$

As a simple choice, we assume that

$$\rho = \rho_0 - \alpha(y_0 - y)^\gamma, \quad \alpha > 0, \quad 0 < \gamma < 1, \tag{4.35}$$

where α and γ are given constants. Near the boundary $y = y_0$, we have the finite difference

$$\Delta\rho \sim \alpha\gamma(y_0 - y)^\gamma. \tag{4.36}$$

Accordingly, the averaged potential vorticity from (4.28) is

$$q = -f_0\Delta\rho/\Delta z = f_0 g\alpha\gamma(y_0 - y)^\gamma/B_\rho{}^0$$
$$= f_0\alpha\gamma(y_0 - y)^{\gamma-1}(g\rho_z{}^a/6\rho_0\beta w_d)^{1/3}(x_e - x)^{-1/3}. \tag{4.37}$$

Therefore, if the density distribution is in the form of (4.35), potential vorticity is infinite near $y = y_0$, and the model is self-consistent.

Obviously, constraint (4.34) or (4.35) applies only to the neighborhood of $y = y_0$. Far away from $y = y_0$, the upper surface density distribution is not subjected to the same constraint.

Since a solution of the ideal-fluid thermocline also depends on the potential vorticity specified for the shallow unventilated thermocline, we have been unable to pin down the range of γ in (4.35). $\gamma = 0.5$ is chosen for a numerical example in section 5.

(ii) In the above discussion, the Ekman pumping velocity is assumed to be a linear function of y near $y = y_0$, see (4.26). If we assume ρ_s remains a linear function of y but w_e has a functional form

$$w_e = w_d(y_0 - y)^\eta, \quad \eta > 1 \quad \text{near} \quad y = y_0, \tag{4.38}$$

then the corresponding dynamic fields near $y = y_0$ have the following estimations

$$B_\rho{}^0 \sim (y_0 - y)^{(\eta+2)/3} \to 0 \quad \text{as} \quad y \to y_0, \tag{4.39a}$$

$$B_\rho{}^b \sim (y_0 - y)^{(\eta-1)/3} \to 0 \quad \text{as} \quad y \to y_0, \tag{4.39b}$$

$$B^0 \sim (y_0 - y)^{(2\eta+1)/3} \to 0 \quad \text{as} \quad y \to y_0, \tag{4.39c}$$

$$u^0 \sim (y_0 - y)^{2(\eta-1)/3} \to 0 \quad \text{as} \quad y \to y_0, \tag{4.39d}$$

$$q \sim -(y_0 - y)^{(1-\eta)/3} \to -\infty \quad \text{as} \quad y \to y_0. \quad (4.39e)$$

Although the inconsistency with the potential vorticity field disappears, the longitudinal velocity on the upper surface vanishes and the base of the moving water outcrops at $y = y_0$. Therefore, this is not a good choice.

(iii) We have assumed that the potential vorticity of the unventilated thermocline matches that of the abyssal water at $y = y_0$, see (4.2). This assumption may not be true for the general case. Suppose that

$$q^h \neq q^a \quad \text{at} \quad y = y_0, \quad (4.40)$$

the upper surface density has a form

$$\rho = \rho_0 - \alpha(y_0 - y)^\gamma, \quad \alpha > 0, \quad 0 < \gamma < \gamma_0 \quad (4.41)$$

and w_e remains the same as in (4.26). After similar manipulations as above, we have the following estimations

$$B_\rho{}^0 \sim (y_0 - y)^{1/3} \to 0 \quad \text{as} \quad y \to y_0, \quad (4.42a)$$

$$B_\rho{}^b \sim (y_0 - y)^{1/3} \to 0 \quad \text{as} \quad y \to y_0, \quad (4.42b)$$

$$B^0 \sim (y_0 - y)^{2/3} \to 0 \quad \text{as} \quad y \to y_0, \quad (4.42c)$$

$$u^0 \sim (y_0 - y)^{-1/3} \to \infty \quad \text{as} \quad y \to y_0, \quad (4.42d)$$

$$q \sim (y_0 - y)^{\gamma - 1/3} \quad \text{as} \quad y \to y_0. \quad (4.42e)$$

Therefore, the consistency of the potential vorticity field requires

$$\gamma < \gamma_0 = \frac{1}{3}. \quad (4.43)$$

When (4.43) is satisfied, the solution is self-consistent. Note that u is unbounded near $y = y_0$, but this is consistent with (4.42b), which means the base of the moving water outcrops at $y = y_0$ and thus the longitudinal velocity must be unbounded.

Our discussion above is based upon the assumption that $\rho_z{}^a$ and q^h are constant. This is not true for general cases. That $q^h \neq q^a$ at $y = y_0$ can introduce some interesting flow patterns which are left for further study.

(iv) The last and the most reasonable choice is to change the eastern boundary condition. If we give up the strict eastern boundary condition that $u \equiv 0$ at $x = x_e$, then q can be finite for water with $\rho < \rho_0$, and there is no inconsistency in our model. A general eastern boundary condition will also make a further constraint on surface density, such as (4.34), (4.35), unnecessary. The detailed discussion will be presented in section 6.

5. A numerical example

We have chosen a model ocean with parameters similar to the North Atlantic Ocean. The model ocean has horizontal scales of $L_x = 6000$ km, $L_y = 6600$ km. The central latitude is at 45°N, thus $f_0 = 0.000103\ s^{-1}$, $\beta = 1.61 \times 10^{-13}\ s^{-1}\ cm^{-1}$. The Ekman pumping velocity has a simple form

$$w_e = -0.0001 \times \sin(2\pi y/L_y), \quad (5.1)$$

where $y = 0$ at the southern boundary. The upper surface density distribution in the subtropical gyre is

$$\rho_s = 1.0274 - 0.0012[2(y_0 - y)/L_y]^{1/2}, \quad (5.2)$$

see the lower part of Fig. 3. Figure 3 also shows the upper surface density map of the subpolar basin. Starting from the southern, eastern and northern boundaries, dense isopycnals gradually outcrop toward the center of the gyre. From (4.23) the outcropping lines are

$$x = x_e + \text{constant}/(f - f_0)^2 w_e. \quad (5.3)$$

It should be noted that the mixed layer in the model is purely passive, i.e., there is no convective adjustment or other type of coupling between the mixed layer and water below. A simple model including convective adjustment is discussed by Huang (1988a).

The stagnant abyssal water has a linear stratification:

$$\rho_z{}^a = -10^{-8}\ \text{g cm}^{-4}. \quad (5.4)$$

As pointed out in the previous section, the deep unventilated thermocline is assumed to have a constant potential vorticity

$$q^h = f\rho_z{}^h = f_0\rho_z{}^a. \quad (5.5)$$

Thus, the stratification of the deep unventilated thermocline varies with the latitude

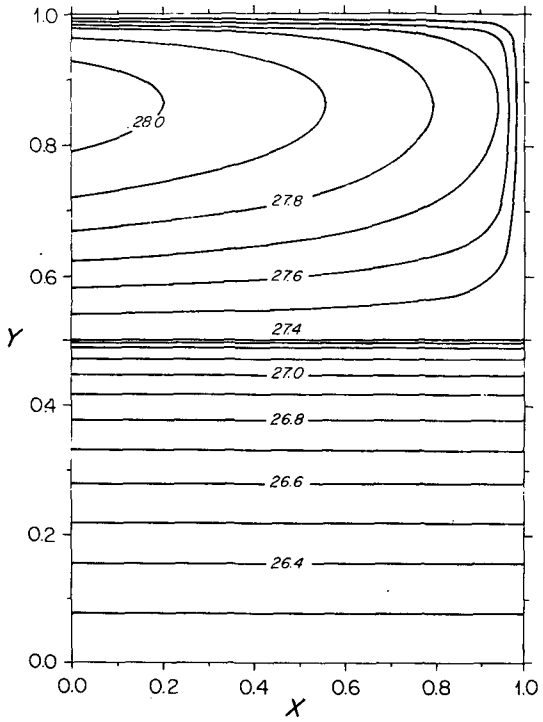

FIG. 3. Upper surface density (σ_θ) distribution in a subtropical–subpolar basin.

$$\rho_z^h = f_0\rho_z^a/f(y), \tag{5.6}$$

where

$$f(y) = f_0 + \beta(y - y_0). \tag{5.7}$$

For the shallow unventilated thermocline, the potential vorticity function can be quite different from the deep unventilated thermocline. We choose the following forms

$$d = d(B_w^s, \rho_i)\{1 + 4 \times \tanh[0.12(B - B_w^s)/B_w^s]\} \tag{5.8}$$

where

$$d = q^{-1} \tag{5.9}$$

is the potential thickness, B_w^s is the upper surface Bernoulli function at the western boundary, ρ_i is the upper surface density of the ith section. We choose such a form based on the following consideration. First, the water in the shallow unventilated thermocline is unlikely to have potential vorticity homogenized. Second, a constant potential vorticity for the shallow unventilated thermocline may introduce some kind of discontinuity into the solution which is an unnecessary complexity in the model. Since the real boundary between the ventilated and unventilated thermocline is unknown before solving the problem, the form in (5.8) can automatically guarantee a smooth transition between these two regions. Anyway, we want to emphasize that the specific form of the potential vorticity functions in (5.8) is technical rather than essential. Different coefficients and form of function can be used positively. The most important point is that the choice of the potential vorticity function of the shallow unventilated thermocline is an important part of formulating a suitable boundary value problem. Although the vertically-integrated mass flux of the wind-driven circulation in a basin is solely determined by the Ekman pumping velocity, the vertical structure of the circulation is determined by many other boundary conditions, such as the sea surface density distribution and the potential vorticity distribution of the deep and shallow unventilated thermocline. Correctly specified boundary conditions determine a unique solution among infinitely many possible solutions.

Since our main goal is to demonstrate the idea rather than numerical detail, a very coarse grid is used for the subtropical basin. The subtropical surface is divided into 12 sections with 21 stations set up along each section. The integration of (2.13) is carried out with a simple Heun scheme and the integral in (4.13) is calculated by a trapezoidal rule.

Both boundary value problem A′ and B′ have been tested numerically. Boundary value problem A′ has been found not very stable. This numerical instability seems largely due to the specific eastern boundary condition used in the model. Since all isopycnals of $\rho < \rho_0$ have to outcrop along the eastern boundary, both v and B_x are singular at $x = x_e$. Because in boundary value problem A′ integration must start from the station adjacent to the eastern wall and move westward station by station, errors accumulate quickly. Therefore, improper treatment of the eastern boundary region leads to a totally unacceptable solution.

Boundary value problem B′ has been found to be rather stable. There are some advantages in this formulation. First, the vertically integrated condition is free of singularity even along the eastern wall. Second, integration at each station is independent of other stations at the same zonal section. Therefore, errors do not accumulate during the integration along one section. The result shown below is calculated with boundary value problem B′.

Since the present example is an extension of the PY model, many results are very similar to their results, with the major exception of the ventilated thermocline. Thus the reader is advised to compare the present results with theirs. In the following discussion only the differences between the two models will be emphasized.

Figure 4 shows the upper surface Bernoulli function map. There is an anticyclonic gyre in the subtropical basin and a cyclonic gyre in the subpolar basin. These two gyres are separated by the intergyre boundary $y = y_0$ along which the zonal velocity is a maximum. By (4.31) one finds

$$u = 4.25(\Delta x)^{2/3} \text{ cm s}^{-1} \tag{5.10}$$

where Δx is the nondimensional distance from the

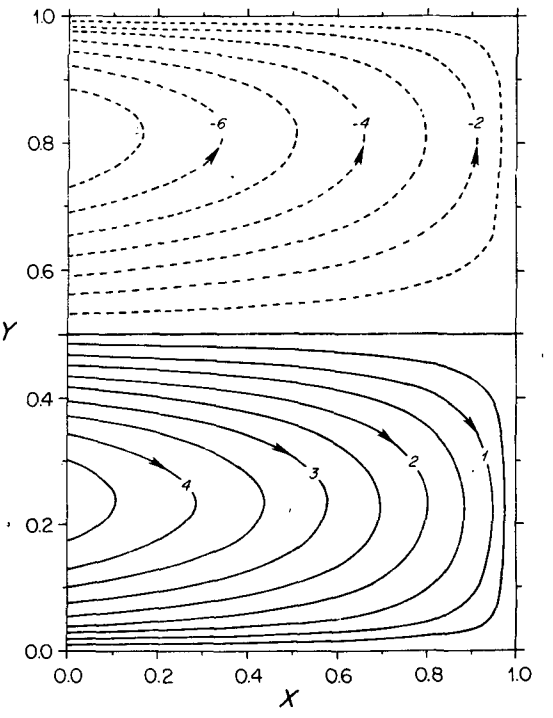

FIG. 4. The upper surface Bernoulli function map of a subtropical-subpolar basin, in units of 10^4 g cm^{-1} s^{-2}.

eastern wall. This velocity value seems on the low side. In HH, u_{max} is the order of 8 cm s^{-1}. This difference is due to the fact that the base of the moving water in the model is very deep. Streamlines are closely spaced along both the eastern and northern boundary, indicating some singularity associated with the velocity field. From (4.22) we can calculate the meridional velocity in the subpolar gyre

$$v^s = B_x^s/f\rho_0 = -0.5[36(f - f_0) \times g\rho_z{}^a w_e{}^2 \beta^{-2}]^{1/3}(x_e - x)^{-1/3}. \quad (5.11)$$

Thus, near the eastern boundary the meridional velocity has an algebraic singularity. Similarly, if we use an approximation

$$w_e = w_d(y - y_n) \quad (5.12)$$

to estimate zonal velocity at the northern boundary, we have

$$u_n^s = -B_y^s/f\rho_0 = -\frac{1}{3}[36(f_n - f_0)g\rho_z{}^a w_d{}^2 \times (x_e - x)^2\beta^{-2}]^{1/3}(y - y_n)^{-1/3}. \quad (5.13)$$

Therefore, both northern and eastern boundaries are algebraic singularity lines for velocity. Although we have not analyzed the eastern and southern boundaries of the subtropical gyre, the structure seems similar. This singularity along these boundaries is an unrealistic feature of the model. For different models the nature of these boundary currents may be different. If the $u \equiv 0$ condition at the eastern boundary is released, ventilated isopycnals need not outcrop along the eastern boundary, and thus the singularity along these boundaries will disappear (Huang, 1988b).

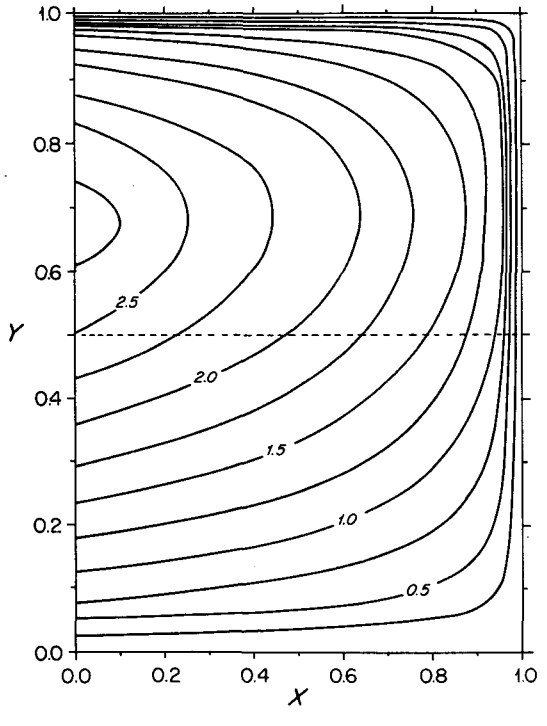

FIG. 5. The base of the moving water, in units of km.

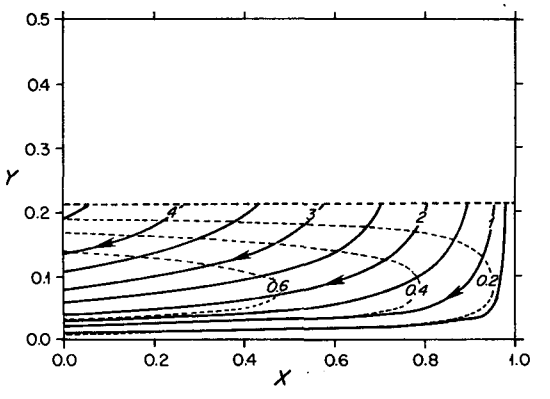

FIG. 6. Flow pattern on isopycnal surface σ_θ = 26.48. Solid lines are streamlines (Bernoulli function isolines, in units of 10^4 g cm^{-1} s^{-2}). Thin dashed lines are depth contours, in units of 100 m. Heavy dashed line is the outcropping line.

For a long time the appropriate lower boundary conditions for the ideal-fluid thermocline have been unclear. Olbers and Willebrand (1984) tried to prove the nonexistence of the level of no motion. However, since potential vorticity and Bernoulli function conservation relations are only meaningful for the moving water, their argument does not apply to the base of the moving water. The present model assumes that the solution should match the stagnant abyssal water at the base of the moving water. Figure 5 shows the depth map of the base of the moving water. Therefore, we have proved the existence of the level of no motion by constructing a solution with the base of the moving water below which every surface is a level of no motion.

As shown in section 4, the solution is continuous across the intergyre boundary. As seen from Fig. 5, the base of the moving water in the subtropical gyre is deepest at the northern edge of the gyre and it increases farther northward. This northern intensification is consistent with observation (i.e., Montgomery, 1938) and the theory of potential vorticity homogenization by RY.

In the following paragraph we discuss flow patterns on different isopycnal surfaces. Figure 6 shows flow patterns on σ_θ = 26.48 surface. This is a very shallow isopycnal surface which outcrops at y = 0.208. Water particles are injected from the mixed layer along the outcropping line and move southwestward toward the western boundary. Since vertical velocity is always negative in the subtropical gyre, streamlines flow from shallow to deep places. Along the southern boundary closely spaced streamlines and isobaths indicate the singularity associated with the boundary. Obviously, all water on this isopycnal surface is ventilated.

The flow pattern on σ_θ = 26.8 is shown in Fig. 7.

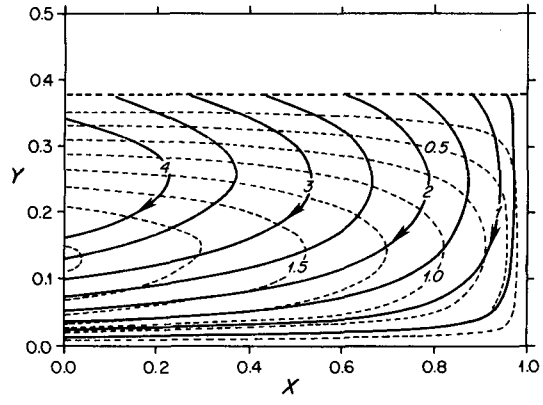

FIG. 7. As in Fig. 6 but on isopycnal surface $\sigma_\theta = 26.8$.

This isopycnal surface outcrops in the northern part of the subtropical basin. After leaving the mixed layer, water particles follow anticyclonic paths, i.e., first move southeastward then southwestward. Along trajectories water particles sink down gradually as seen by the intersection of the trajectories with the isobaths. In the northwest corner there is water coming from the western boundary outflow. This is the so-called shallow unventilated thermocline, or the pool region in LPS. Note that the boundary between the ventilated and shallow unventilated thermoclines is a result of global dynamic balance. It was unknown before the solution was found. It is the special feature of the ideal-fluid thermocline equation. This solution-dependence of the boundary is not unlike the sonic line (where the local particle velocity is equal to the local sound velocity) in transonic aerodynamics, which must be calculated as part of the solution and different boundary conditions must apply to different sides of this critical line.

Figure 8 shows the flow pattern on $\sigma_\theta = 27.4$. This isopycnal surface outcrops along the intergyre boundary. Complete anticyclonic trajectories on this isopycnal surface are a typical pattern for a subtropical gyre. All water particles on this surface are unventilated. In the model this surface is the interface between the deep and shallow unventilated thermoclines. As shown in the previous section, potential vorticity of the shallow unventilated thermocline must be infinite near the northern edge of the subtropical gyre; therefore, the potential vorticity has some kind of discontinuity across this surface. Of course, if the no-flux eastern boundary condition is released, it may be possible to construct a solution which has potential vorticity continuous across this interface.

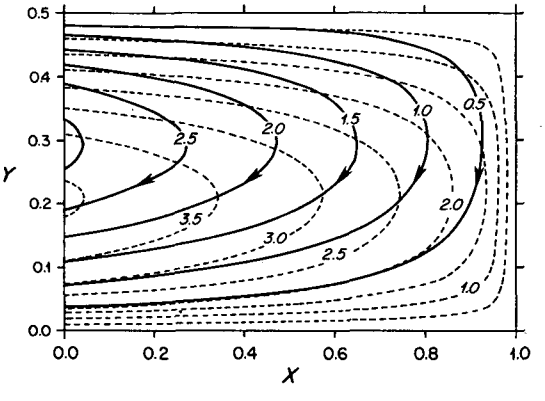

FIG. 8. As in Fig. 6 but on isopycnal surface $\sigma_\theta = 27.4$.

For isopycnal surfaces with $\sigma_\theta > 27.4$, their patterns are different. These isopycnals extend into the subpolar basin and some of them outcrop.

Figure 9 shows the flow pattern on $\sigma_\theta = 27.8$. This isopycnal surface outcrops in the middle of the subpolar basin, shown by the heavy dashed line. In the subpolar gyre streamlines emerge from the western boundary with given potential vorticity and move upward along cyclonic trajectories until they reach the outcropping line where they are picked up by the mixed layer. Note that a small part of the water on this isopycnal surface does not outcrop, but comes back to the western boundary at the northwestern corner. Along the edge of the northern, southern, and eastern boundaries there is a narrow band of stagnant abyssal water (shadow zone in LPS). There is an anticyclonic gyre in the sub-

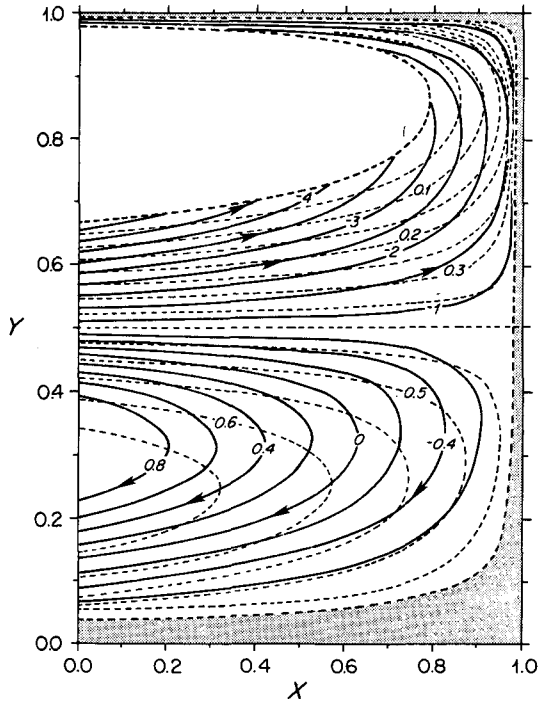

FIG. 9. Flow pattern on isopycnal surface $\sigma_\theta = 27.8$. Shaded area is the shadow zone and the heavy dashed line is the base of the moving water. Solid lines are Bernoulli function isolines, in units of 10^4 g cm^{-4} s^{-2}. Thin dashed lines are depth contours, in units of km. The innermost dashed line in the subpolar basin is the outcropping line.

tropical basin. Comparing isobaths in Figures 6, 7, 8, 9 (and 10), it is readily seen that the bottom of each isopycnal surface is gradually moving toward the northern boundary of the subtropical gyre, i.e., the so-called northern intensification.

Figure 10 shows the flow pattern on $\sigma_\theta = 28.9$. (We realize that σ_θ in the real oceans never reaches such a high value. Since a linear stratification has been used in the example, this isopycnal surface just shows an example for the deep unventilated thermocline.) This isopycnal surface does not outcrop, and there is a vast domain of stagnant abyssal water. The intersection of the base of the moving water and this isopycnal surface is shown as a heavy dashed line. The isobath map shows a dome-shaped structure in the subpolar basin and a small bowl-shaped structure in the subtropical basin. At this density surface the subtropical gyre has been reduced to a very tight circulation in the northwestern corner of the subtropical basin.

The vertical structure of the circulation can be seen clearly from different vertical sections. Figure 11 shows a zonal section across the central latitude of the subtropical gyre ($y = 0.25$). All isopycnals with $\rho < \rho_0$ outcrop at the eastern boundary. Therefore, all these density layers reduce to zero thickness, corresponding to an infinite potential vorticity. This singularity is intrinsic for the eastern boundary condition used in the present model. If another type of eastern boundary condition is used, the structure near the eastern boundary may be different. Below the ρ_0 isopycnal surface there is the deep unventilated thermocline with a constant potential vorticity and the stagnant abyssal water. A heavy dashed line indicates the boundary between these two types of water (the base of the moving water).

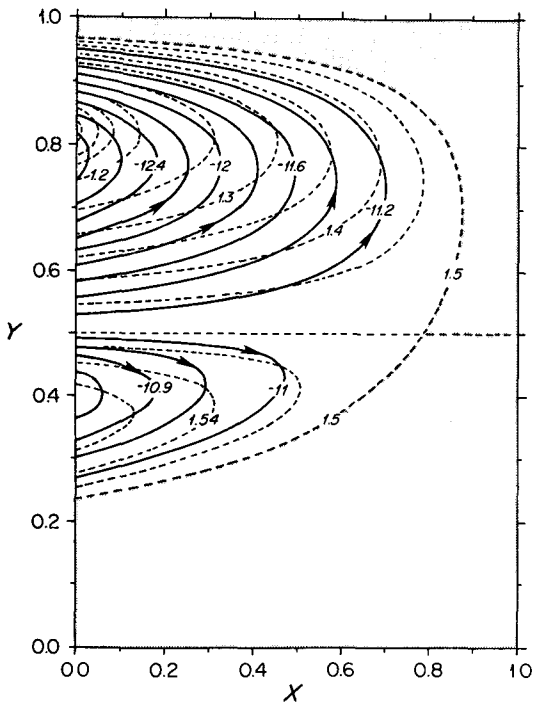

FIG. 10. As in Fig. 9 but on isopycnal surface $\sigma_\theta = 28.9$.

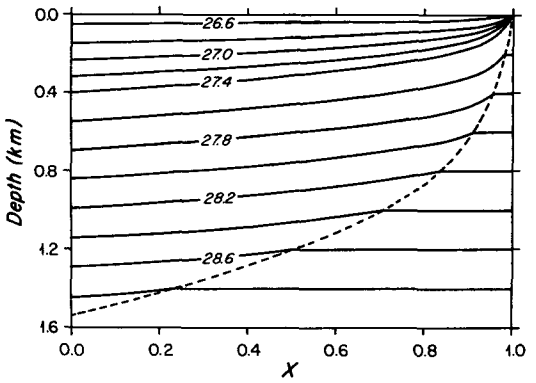

FIG. 11. Density section at $y = 0.25$. Dashed line is the base of the moving water, stagnant abyssal water is on the right and the deep unventilated thermocline is on the left. Note that below the $\sigma_\theta = 27.4$ isopycnal surface the density interval is double.

The density section at the central latitude of the subpolar basin is shown in Fig. 12. The same figure was shown by PY. We include this figure to make our circulation complete. Here all moving water has the same potential vorticity, some shallow isopycnals outcrop, while others do not. A dashed line indicates the boundary between the moving and stagnant water.

The density section at the western boundary is shown in Fig. 13. In the upper part of the subtropical gyre, there is the ventilated thermocline and the shallow unventilated thermocline. This part of the map is the essential difference between the model and PY's solution. A heavy dashed line indicates the base of the moving water. Obviously, the bottom of the moving water reaches the maximum in the middle of the subpolar western boundary. In the subtropical basin the bottom

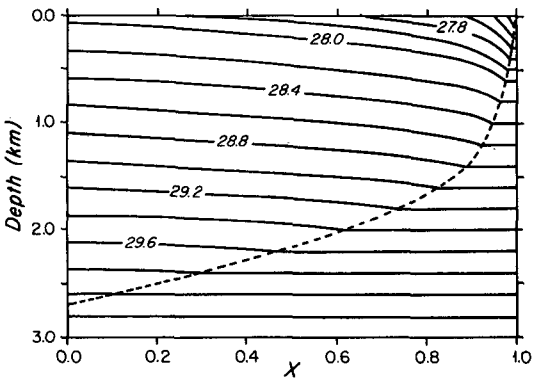

FIG. 12. Density section at $y = 0.75$. Dashed line is the base of the moving water. Isopycnal interval is double for the no-outcropping isopycnals.

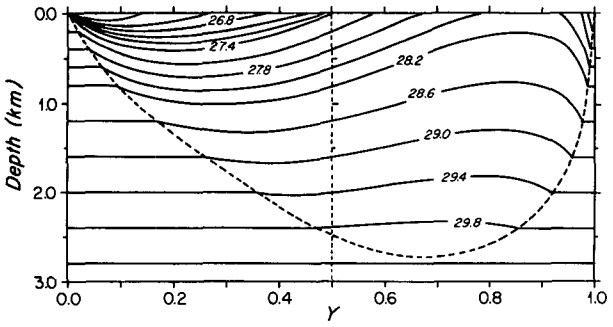

FIG. 13. Density section at the western boundary. Heavy dashed line is the base of the moving water, thin dashed line is the intergyre boundary. Isopycnal interval is double for non-outcropping isopycnals.

of the isopycnal surface gradually moves northward and reaches a depth of 2.5 km at the northern edge of the subtropical basin. This is the northern intensification of the subtropical gyre.

As a comparison, we have included a σ_θ-section from the western North Atlantic (GEOSECS), Fig. 14. Since our model includes neither mixed layer nor thermohaline process, we will compare the structure between the 100 and 2000 m depth. Here we see the stagnant abyssal water separating from the moving water by an interface deepening northward, thus leaving a vast zone of stagnant water in the equatorial region. Near the intergyre boundary, there is a fairly sharp horizontal density front representing the Gulf Stream. Therefore, assuming an infinite density gradient in the model is a reasonable approximation in this area. There are clearly bowl-shaped isopycnals in the subtropical gyre and dome-shaped in the subpolar gyre. Our model seems able to reproduce the overall structure of the subtropical gyre, especially the top 1000 meters. However, the model result is quite different from the observation for the deep circulation and the subpolar gyre, due to our basic assumption of nondirect thermal forcing and linear stratification of the abyssal water. Since our focus in this study is mainly on the basic formulation of boundary value problems of the thermocline equation rather than comparison with observations, we will not try to go into the details.

Another way of viewing the continuous circulation structure is the β-spiral method. We have drawn two β-spiral diagrams. Figure 15 shows four spiral diagrams in the subtropical gyre. Some marks on the curves are not equally spaced near the upper surface, but marks for the deep unventilated thermocline show vertical stations with a density interval of $\Delta\sigma_\theta = 0.1$. These curves clearly show the continuous vertical structure. All these curves converge at the coordinate origin, confirming the existence of the base of the moving water. Below the upper surface $\partial u/\partial z$ is always negative due

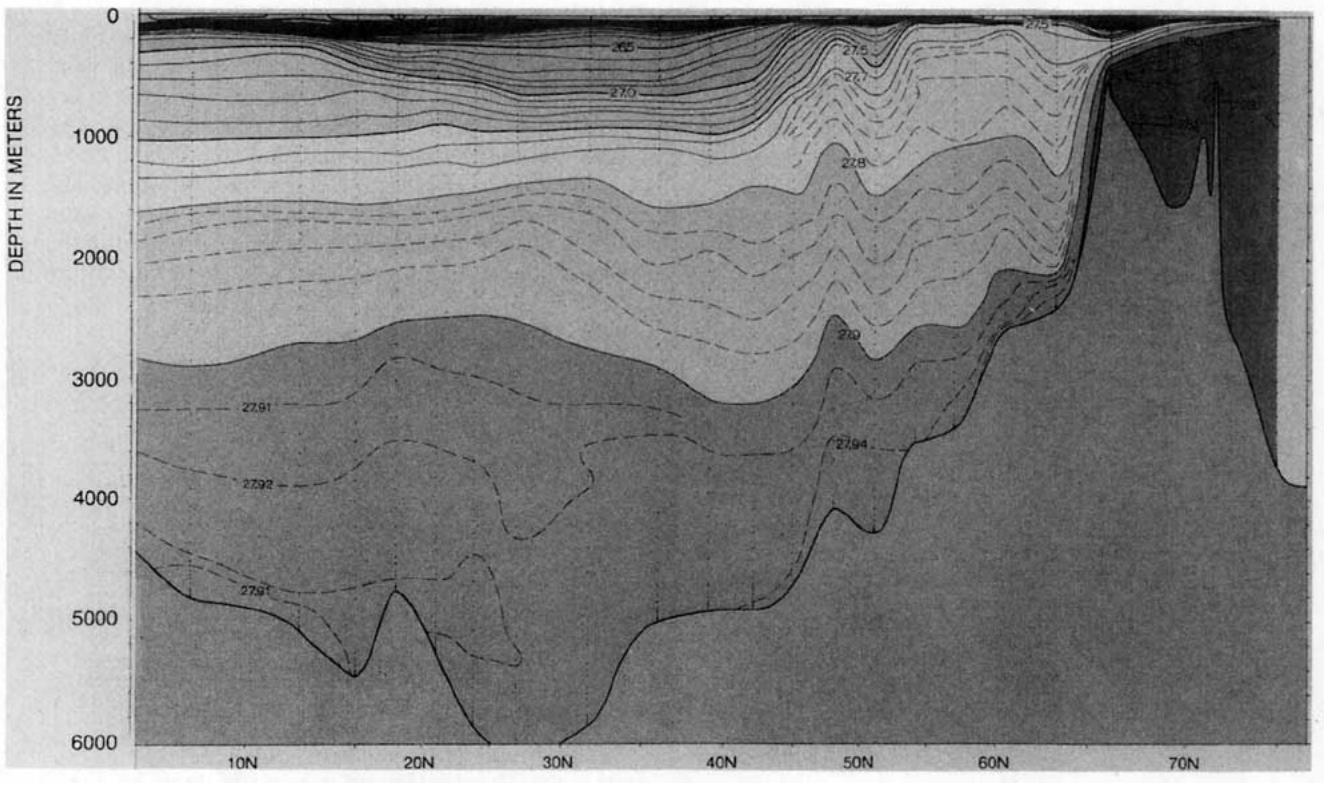

FIG. 14. A σ_θ-section of the western North Atlantic. (Adapted from GEOSECS Atlantic Expedition.)

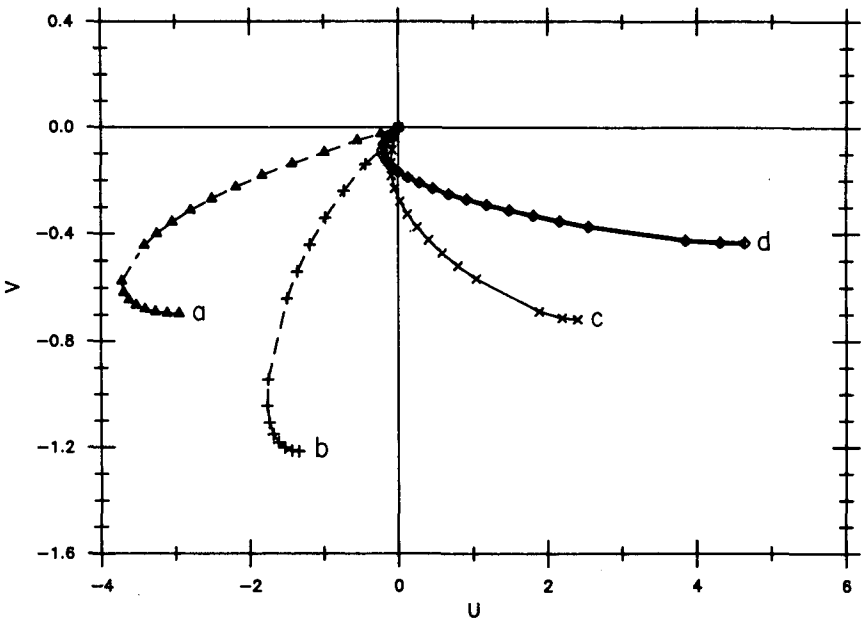

FIG. 15. Beta-spirals in the subtropical gyre (in units of cm s^{-1}) at points, (x, y)-coordinates: (a) 0.25, 0.125; (b) 0.75, 0.125; (c) 0.75, 0.375; (d) 0.25, 0.375.

to the thermal wind relation. Accordingly, the zonal velocity may reach a maximum value below the surface as indicated by curves (a) and (b). Near the base of the moving water all u-components become negative. This is due to the fact that the bottom of the isopycnals migrates northward, thus at any point in the subtropical gyre the velocity at the lowest moving isopycnal is always westward.

Figure 16 shows four β-spirals in the subpolar basin which have structure similar to the previous case, ex-

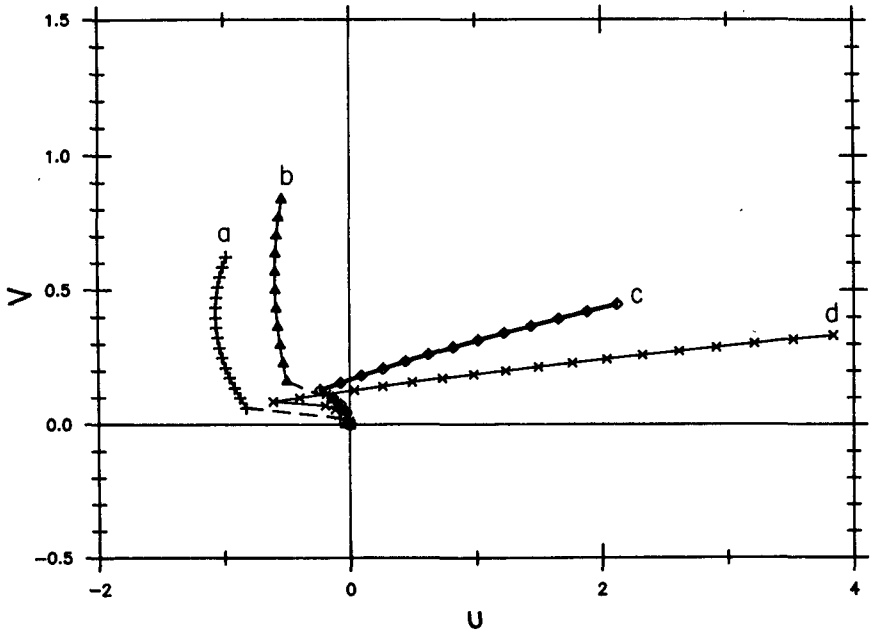

FIG. 16. Beta-spirals in the subpolar gyre (in units of cm s^{-1}) at (a) 0.25, 0.875; (b) 0.75, 0.875; (c) 0.75, 0.625; (d) 0.25, 0.625.

cept now the spirals rotate in the opposite direction. These curves are not very smooth near the base of the moving water due to the very low resolution used in the calculation.

Since there have been many similarity solutions, which are based upon specific assumptions, a natural question is how does the present solution compare with some existing similarity solutions. We have shown the functional relation between the potential vorticity and the Bernoulli function, Fig. 17. Since the potential vorticity is infinite along the eastern boundary, it is easy to use the reciprocal $d = q^{-1}$ in the calculation. This quantity can be called potential thickness. Therefore, the *d-B* relation is the actual relation shown in Fig. 17. In many similarity solution studies, d has an assumed simple form. For example, Killworth (1987) assumes

$$d = F(\rho)B.$$

This relation corresponds to a straight line from the coordinates' origin. Obviously, our solution is quite different from the above assumption.

In fact, the major point in this study is that the potential vorticity of the ventilated thermocline is a solution of a complete boundary value problem of the ideal-fluid thermocline equation. Different boundary conditions will certainly give different forms of potential vorticity function for the ventilated thermocline. Any a priori specified form of this function cannot satisfy a general form of boundary condition.

As the final step, we show the potential vorticity map on the upper surface of the subtropical basin in Fig. 18. We leave the band along the northern, eastern, and southern boundaries blank since potential vorticity along these boundaries is infinite. Potential vorticity is finite and continuous away from these boundaries, thus our continuous model is free of the potential vorticity singularity along the outcropping lines in the LPS model.

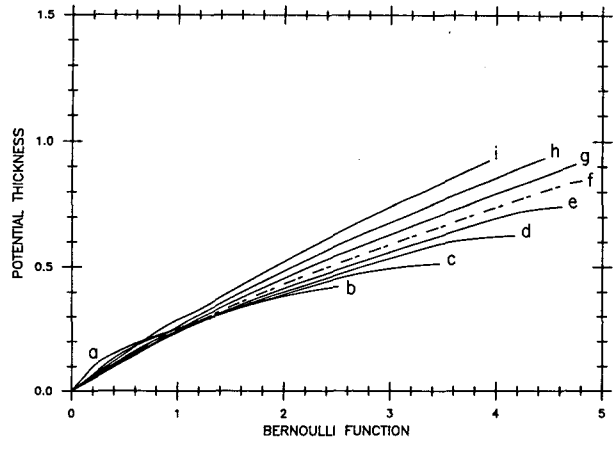

FIG. 17. Potential thickness (in units of 10^{12} g^{-1} cm^4 s)-Bernoulli function (in units of 10^4 g cm^{-1} s^{-2}) relations for different densities: (a) $\sigma_{\theta 1}$ = 27.05, (b) $\sigma_{\theta 2}$ = 26.91, (c) $\sigma_{\theta 3}$ = 26.8, (d) $\sigma_{\theta 4}$ = 26.71, (e) $\sigma_{\theta 5}$ = 26.63, (f) $\sigma_{\theta 6}$ = 26.55, (g) $\sigma_{\theta 7}$ = 26.48, (h) $\sigma_{\theta 8}$ = 26.42, (i) $\sigma_{\theta 9}$ = 26.36.

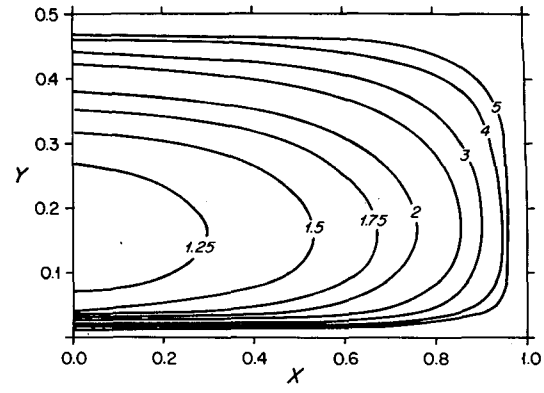

FIG. 18. Potential vorticity distribution on the upper surface, in units of 10^{-12} g cm^{-4} s^{-1}. The value should have been ∞ at the northern, eastern and southern edges.

6. General boundary value problems for subtropical/subpolar basins

a. The general case when $\rho_s = \rho_s(x, y)$ in the subtropical basin

Assume that the northern boundary of the subtropical basin is still a latitude line $y = y_0$ where $w_e = 0$ and ρ_s = constant. According to a lemma proved by HH, a solution with no-mass-flux crossing $y = y_0$ is a consistent solution and thus the subtropical basin can be treated in isolation. Then both boundary value problems A and B can be modified as follows.

1) BOUNDARY VALUE PROBLEM A (MODIFIED)

Introducing new orthogonal coordinates (l, n) such that l = constant follow ρ_s = constant lines, (2.29) can be rewritten as

$$v = -w_e(z_\rho d\rho_s/dn)^{-1}. \qquad (2.29')$$

Using the geostrophic condition, one obtains

$$dB^s/dl = -\rho_0 w_e q_s (d\rho_s/dn)^{-1}. \qquad (2.30')$$

Therefore, by tracing along ρ_s = constant lines, the integration process can be carried out similar to before. Examples of tracing surface density contours has been shown by HH.

2) BOUNDARY VALUE PROBLEM B (MODIFIED)

Equation (2.37) is still valid and the formulation of boundary value problem B is basically unchanged. However, instead of creating N one-dimensional data arrays $q = Q_i(B, \rho_i)$ $(i = 1, \cdots, N)$, now we generate a two-dimensional array $q = Q(B, \rho)$ at irregular points (B_i, ρ_i) $(i = 1, \cdots)$. In the process of integration,

potential vorticity is calculated by interpolation of this two-dimensional array. There might be some ambiguity about the exact boundary separating the ventilated thermocline from the shallow unventilated thermocline in the (B, ρ) space. Otherwise, the integration procedure remains the same as before. This problem will be reported in some upcoming study.

b. Lemma condition

A lemma proved by HH guarantees that there is no closed ρ_s = constant line in a subtropical basin. Thus boundary value problems A and B can always be solved in the general case.

c. General eastern boundary condition

As shown in section 4, strictly requiring

$$u \equiv 0$$

at the eastern boundary introduces some kind of singularity in the solution, such as

(i) both v and q are infinite near the eastern boundary;
(ii) the upper surface density distribution is subject to a consistent condition (4.34).

These features seem unrealistic and thus general eastern boundary conditions may be useful for a more realistic model of the ideal-fluid thermocline. Since an exact formulation of the general eastern boundary condition requires detailed analysis of some possible mixing/friction mechanism, we will tentatively formulate our eastern boundary condition as follows:

The general eastern boundary condition: the stratification at the eastern wall is

$$B^e = \begin{cases} B^e(y, \rho), & \rho \leqslant \rho_b(y), \\ B^a(\rho), & \rho \geqslant \rho_b(y) \end{cases} \tag{6.1}$$

such that

$$\int_{z_b}^{0} u dz \equiv 0 \tag{6.2}$$

where z_b is the depth of the ρ_b-isopycnal, B^e and B_ρ^e are continuous at $\rho = \rho_b$. So far we have not studied the structure of such an eastern boundary current which can set up the stratification described above. This problem calls for close investigation of the eastern boundary currents.

We specify the water property along the entire eastern boundary regardless of whether the water is coming or going out of the boundary. This assumption implies potential mixing within the eastern boundary current which can change the water properties.

For the general eastern boundary condition, (2.37) has to be modified

$$-\int_{\rho_s}^{\rho_b} B_\rho{}^2 d\rho + \int_{\rho_s}^{\rho_b} B_\rho{}^{e^2} d\rho = 2\rho_0 f^2 g/\beta \cdot \int_x^{x_e} w_e dx + \int_x^{x_e} B_\rho{}^2(\rho_b) d\rho_b/dx \cdot dx, \tag{6.3}$$

where the second term on the left-hand-side is a contribution from the general eastern boundary condition.

Now boundary value problem B can be carried out the same way as above and boundary value problem A has the same formulae as above.

Obviously, all these singular features of the solutions, i.e., unbound meridional velocity and potential vorticity at the eastern boundary and the consistent constraint on the upper surface density, do not appear for general eastern boundary conditions. In a sense, we have removed all the singularities from the interior to the eastern boundary current. Admittedly, different eastern boundary conditions will lead to different interior solutions. Further study is vitally important in order to understand the eastern boundary current structure and its influence over the interior dynamics (Huang, 1988b).

d. Mixed layer assumed passive

A passive mixed layer assumption means the mixed layer pumps water down with given density distribution in the subtropical gyre and picks up water in the subpolar gyre regardless of the water temperature. There is no interaction between the mixed layer and the water below otherwise. Coupling the model to include convective adjustment in a subpolar gyre is discussed in a separate paper (Huang, 1988a), and a model including a mixed layer is under study currently.

e. Inversion problems for subtropical/subpolar gyres

As pointed out by HH, the ideal-fluid thermocline equation is a low order (non-strict) hyperbolic system. Therefore, information can propagate upstream or downstream along streamlines. Apparently, the surface density ρ_s in the subpolar basin can be measured easily, thus we may try to use ρ_s and w_e as given upper boundary conditions and apply boundary value problem A or B for a subpolar basin. Namely, assume w_e, ρ_s and $q = q(B, \rho)$ for $\rho > \rho_n$ (the upper surface density at the northern boundary of the subpolar gyre) are given, we may calculate $q = q(B, \rho)$ for $\rho < \rho_n$ by tracing the streamline backward.

Similarly, assume that $q(B, \rho)$ is given for all water particles in the subtropical gyre, boundary value problem C can be solved and ρ_s is found as the "outcropping" isopycnal by tracing backward along streamlines.

Although this kind of inverse problem seems physically strange, it is an inescapable mathematical result of the simplification implied by the basic assumption with the ideal-fluid thermocline equation. The usefulness of this inversion process needs further study.

7. Conclusion

The major new contribution in this study is formulating and solving boundary value problems for the ideal-fluid thermocline equation. Using a lemma proved by HH, a two-gyre basin is divided into two regions with different signs of Ekman pumping velocity and different boundary value problems have been formulated accordingly. Therefore, the problem of solving the nonlinear ideal-fluid thermocline equation is reduced to repeatedly integrating a second-order ordinary differential equation with free boundary conditions. These boundary value problems are deterministic, thus for reasonably given boundary conditions, they have sound solutions.

Traditionally, the homogeneous or reduced gravity wind-driven ocean circulation models totally ignore the influence of the western boundary current. The western boundary current is at most a passive part of the general circulation which can be solved and patched together with the interior solution *after* the entire interior solution has been determined. Consequently, the dynamic role of the western boundary was largely untouched.

Our model also excludes the western boundary current. However, through setting up the density and potential vorticity relation at the western boundary outflow region, the western boundary current implicitly plays a vitally important role in setting up the baroclinic structure of the wind-driven circulation.

Although our model uses the ideal-fluid assumption, the dynamic role of eddy mixing is implicitly included in the model through specification of potential vorticity for the unventilated thermocline.

Likewise, the thermohaline circulation should play a similar role in determining the baroclinic modes of the circulation through setting up the stratification of the abyssal water.

Since the ideal-fluid thermocline equation uses linear momentum equations in the horizontal direction, the vertically-integrated circulation is determined by the classical Sverdrup dynamics as in a homogeneous ocean circulation model. Our model gives concrete ways of determining the barotropic and baroclinic modes of the circulation. In brief, we have shown systematically how the boundary conditions, i.e., the Ekman pumping velocity, the upper surface density, the potential vorticity of the shallow and deep unventilated thermocline, and the stratification of the stagnant abyssal water, determine the entire solution.

For a simple case with constant potential vorticity for the deep unventilated thermocline, the free boundary value problems in the subtropical gyre reduce to fixed boundary value problems of the same second-order ordinary differential equation, while in the subpolar gyre the problem results in a closed analytical solution. We have shown one example with a two-gyre circulation. Our goal here is to demonstrate the main idea, thus a very coarse grid-mesh and simple second-order accuracy scheme have been used. Some better numerical scheme and fine grids could be used in a further study to examine the well-posedness of these boundary value problems.

We have shown the influences of all boundary conditions only in a very abstract way of formulating the boundary value problems. The detailed study of these effects is very important for understanding the general circulation. This study is currently underway and will be published subsequently.

Our study has shown that a no-flux condition at the eastern boundary is associated with some intrinsic singularity. Although we have shown one consistent solution with this kind of boundary condition, further study seems very important to reveal the dynamic role of the general eastern boundary condition.

Admittedly, the ideal-fluid thermocline is a highly idealized theory; many important processes have been omitted, such as mixing in the interior, coupling with the western boundary current, coupling with the thermohaline circulation, and coupling with the mixed layer. Understandably, the ideal-fluid thermocline cannot be solved in isolation. In our model the effects of these high order dynamical processes have been parameterized as some fixed boundary conditions at all these boundaries. Further study is required to modify the ideal-fluid thermocline theory in order to provide a more realistic solution in a closed basin.

Acknowledgments. The basic idea in this study was formulated while I worked in the Geophysical Fluid Dynamics Laboratory at Princeton University as a visiting scientist. Kirk Bryan gave some useful suggestions. The wonderful example of the LPS model and Joe Pedlosky's belief that the problem of the ideal-fluid thermocline can be solved kept me at work. I am grateful for the generous support of the Mellon Advanced Study Award from the Woods Hole Oceanographic Institution and a grant from the National Science Foundation (OCE86-14771).

REFERENCES

Courant, R., and K. O. Friedrichs, 1948: *Supersonic Flow and Shock Waves.* Wiley-Interscience, 484 pp.

Hodnett, P. F., 1978: On the advective model of the thermocline circulation. *J. Mar. Res.*, **36,** 185–198.

Huang, R. X., 1984: The thermocline and current structure in subtropical/subpolar basins. Ph.D. thesis, Massachusetts Institute of Technology and Woods Hole Oceanographic Institution Joint Program in Oceanography, 218 pp.

——, 1986: Solutions of the ideal-fluid thermocline with continuous stratification. *J. Phys. Oceanogr.*, **16,** 39–59.

——, 1988a: Ideal-fluid thermocline with weakly convective adjustment. *J. Phys. Oceanogr.*, **18,** 642–651.

——, 1988b: On the generalized eastern boundary conditions and the three-dimensional structure of the ideal-fluid thermocline. Submitted to *J. Geophys. Res.*

Janowitz, G. S., 1986: A surface density and wind-driven model of the thermocline. *J. Geophys. Res.*, **91,** 5111–5118.

Killworth, P. D., 1987: A continuously stratified nonlinear ventilated thermocline. *J. Phys. Oceanogr.*, **17,** in press.

Luyten, J. R., J. Pedlosky and H. Stommel, 1983: The ventilated thermocline. *J. Phys. Oceanogr.*, **13,** 292–309.

Mesinger, F., and A. Arakawa, 1976: Numerical methods used in atmospheric models. *GARP Publ. Ser. No. 17,* Vol. I, 64 pp.

Montgomery, R. B., 1938: Circulation in the upper layers of southern North Atlantic deduced with use of isentropic analysis. *Pap. Phys. Oceanogr. Meteorol.*, **6,** 55 pp.

Olbers, D. J., and J. Willebrand, 1984: The level of no motion in an ideal fluid. *J. Phys. Oceanogr.*, **14,** 203–212.

Pedlosky, J., and W. R. Young, 1983: Ventilation, potential vorticity homogenization and the structure of the ocean circulation. *J. Phys. Oceanogr.*, **13,** 2020–2037.

Rhines, P. B., 1986: Lecture on ocean circulation dynamics. *Large-Scale Transport Processes in Oceans and Atmosphere.* J. Willebrand and D. L. T. Anderson, Eds., P. Reidel.

——, and W. R. Young, 1982: A theory of the wind-driven circulation. I. Mid-ocean gyres. *J. Mar. Res.*, **40**(Suppl.), 559–596.

Robinson, A. R., 1965: A three-dimensional model of inertial currents in a variable-density ocean. *J. Fluid Mech.*, **21,** 211–223.

——, and H. Stommel, 1959: The oceanic thermocline and the associated thermohaline circulation. *Tellus,* **3,** 295–308.

Veronis, G., 1969: On theoretical models of the thermocline circulation. *Deep-Sea Res.*, **16**(Suppl.), 301–323.

Welander, P., 1959: An advective model of the ocean thermocline. *Tellus,* **11,** 309–318.

——, 1971: Some exact solutions to the equations describing an ideal-fluid thermocline. *J. Mar. Res.*, **29,** 60–68.

Young, W. R., and G. R. Ierley, 1986: Eastern boundary conditions and weak solutions of the ideal thermocline equations. *J. Phys. Oceanogr.*, **16,** 1884–1900.